Neuroimaging of Spine Tumors

Nandor K Pinter MD, Thomas J Pfiffner MD, Laszlo L Mechtler MD

Nandor K Pinter, MD

Neuroimaging Research Fellow, Dent Neurologic Institute, 3980 Sheridan Drive, Amherst NY 14226, USA.

Telephone number: 716-250-2000; Fax number: 716-250-2045

Email address: npinter@dentinstitute.com

Thomas J Pfiffner, MD

Neuro-oncology Fellow, Dent Neurologic Institute, 3980 Sheridan Drive, Amherst NY 14226, USA.

Telephone number: 716-250-2000; Fax number: 716-250-2045

Email address: tpfiffner@dentinstitute.com

Laszlo L Mechtler, MD

Professor of Neurology and Oncology, Dent Neurologic Institute, 3980 Sheridan Drive, Buffalo, NY 14226, USA; Roswell Park Cancer Institute, Buffalo, NY, USA.

Telephone number: 716-250-2000; Fax number: 716-250-2045

Email address: lmechtler@dentinstitute.com

Abstract:

Intramedullary, intradural/extramedullary, and extradural spine tumors comprise a wide range of neoplasms with an even wider range of clinical symptoms and prognostic features. MR imaging, commonly used to evaluate the spine in patients presenting with pain, can further characterize lesions that may be encountered on other imaging studies, such as bone scintigraphy or CT. The advantage of the MRI is its multi-plane capabilities, superior contrast agent resolution, and flexible protocols that play an important role in assessing tumor location, extent in directing biopsy, in planning proper therapy, and in evaluating therapeutic results. A multimodality approach can be used to fully characterize the lesion and the combination of information obtained from the different modalities usually narrows the diagnostic possibilities significantly. The diagnosis of spinal tumors is based on patient age, topographic features of the tumor, and lesion pattern as seen at CT and MR imaging. The shift to high-end imaging incorporating DWI, DTI, MRS, Whole-body STIR, PET, intraoperative and high-field MRI as part of the mainstream clinical imaging protocol has provided neurologists, neuro-oncologists, and neurosurgeons a window of opportunity to assess the biologic behavior of spine neoplasms. This chapter reviews neuroimaging of spine tumors, primary and secondary, discussing routine and newer modalities that can reduce the significant morbidity associated with these neoplasms.

Keywords: MRI, CT, Primary spinal tumors, metastatic spine tumors, meningioma, chordoma, plasmacytoma, nerve sheath tumors, ependymoma, astrocytoma, hemangioblastoma.

Introduction

The historic classification of spine tumors is based on the use of myelography with 3 main groups as schematically depicted in Fig. 1: (1) extramedullary extradural, (2) intradural extramedullary, and (3) intradural intramedullary**.** The incidence of metastatic disease involving the vertebrae, epidural space and leptomeninges accounts for 97% of tumors involving the spine. Primary tumors of the spine, spinal cord, spinal meninges, and cauda equina are relatively rare (Duong 2012). Data from national registries and improved imaging capabilities have allowed spine tumor specialists the opportunity to study and treat these unusual and rare tumors with more confidence and better results. The introduction of MRI to clinical practice has been one of the most important advances in the care of patients with spine tumors. The characterization of spine tumors by MRI involves determining, in the context of patient's age and sex, the location of the lesion and whether or not it enhances after gadolinium injection. CT best delineates osseous integrity while MRI is better at assessing soft tissue involvement. The purpose of this chapter is to describe the neuroimaging findings of spine tumors based on the location of the tumor in its relationship to the dura and spinal cord (Mechtler and Nandigam 2013).

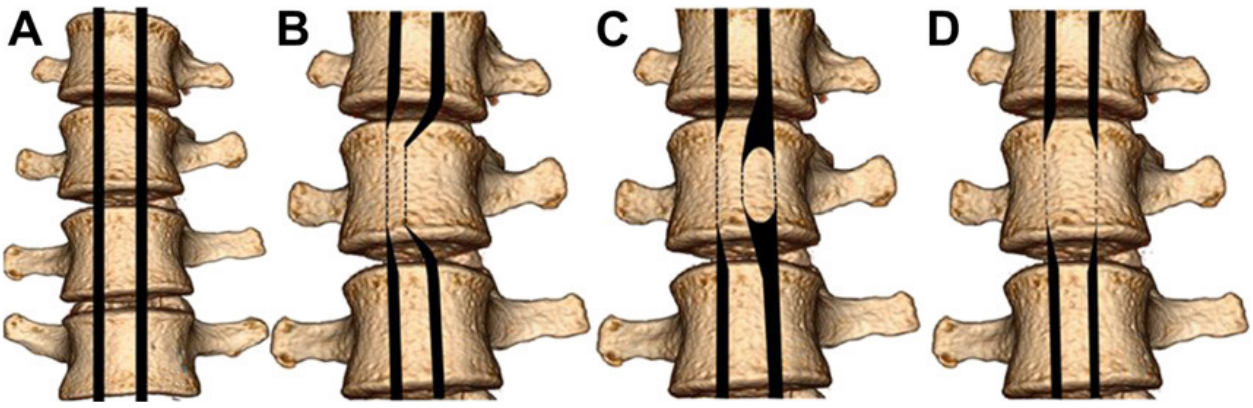

Figure 1. Historic classification of spine tumors based on myelography. (A) Normal, (B) extradural extramedullary, (C) intradural extramedullary,and (D) intradural intramedullary.

METATSTATIC TUMORS OF THE VERTEBRAL COLUMN

The spine is the third most common site for metastatic disease and the most common site for bone metastasis (Shah and Salzman 2011). Metastatic disease of the vertebral column is more frequent than primary neoplastic diseases. Approximately two-third of cancer patients will develop bone metastasis and symptomatic spinal metastasis will occur in almost 10% of cancer patients. The most common primary sites are the prostate, breast, kidney, lung and thyroid. The incidence of skeletal metastases according to the primary tumor are as follows; breast 73% (47-85%), prostate 68% (33-85%), thyroid 42% (28-60%), lung 36% (30-55%), kidney 35% (33-40%), esophageal 6% (5-7%), and gastrointestinal 5% (3-11%) (Maccauro et al 2011) The most common cause of metastatic spine disease is breast cancer in women, however, in men, prostate cancer is most common. The thoracic spine is the most commonly involved. The majority of the lesions are extradural in location, consisting of lesions which are localized to the epidural space and those which are nested in the vertebral body. Prostate, breast and lung cancer are again the leading cause of spinal cord compression, each accounting for about 15-20% of the cases. The remaining cancers stem from renal cell, Non-Hodgkin's lymphoma, multiple myeloma, colorectal cancers, sarcomas and unknown tumors. Pain, the most common initial feature, occurs in 95% of adults and 80% of children. Pain is usually localized to the site of metastasis and is caused by stretching the pain-sensitive bony periosteum. Radicular pain is less frequent but is also localizing. Nocturnal pain upon lying down is typical.

Three types of bone metastasis are distinguished; osteolytic, osteoblastic and mixed; 71% are osteolytic, 8% are osteoblastic, and 21% are mixed. In many cases, a mix of lytic and sclerotic lesions can be found; 71% are osteolytic, 8% are osteoblastic and 21% are mixed. This is a result of osteoclast activation, rather than a direct invasion of bone tissue by tumor cells.

Osteolytic metastases typically develop in cancers of the breast, lung, kidney, thyroid, oropharyngeal cancers (Shah and Salzman, 2011) and in melanoma (Sun et al., 2013).

In osteoblastic metastases the balance of bone metabolism is shifted to the benefit of bone production as a result of pathologic activation of osteoblasts. Osteoblastic lesions usually occur in prostate, bladder and nasopharyngeal cancer, medulloblastoma, neuroblastomas and bronchial carcinoid (Long et al., 2010).

Imaging of vertebral metastases

In today's clinical practice MRI is the most important modality in imaging of metastatic spine disease. Plain film is no longer the routine diagnostic toolbar due to its low sensitivity and specificity (Salvo et al 2009, Shah and Salzman 2011). Nuclear medicine studies have a well-defined role in metastasis imaging. Bone scans have been used for screening, since the tracer accumulates in metastatic sites with high sensitivity, thus reflecting the increased bone turnover. The sensitivity and specificity of bone scans were improved with single photon emission computed tomography (SPECT) scans (Ryan 1995). Flurodeoxyglucose (F18-FDG) positron emission tomography (PET) alone and PET-CT can discover spinal metastases with a sensitivity of 74% and 98%, respectively (Metser et al. 2004). F18-FDG PET has been reported to be more sensitive in detecting osteolytic metastases (Cook and Fogelman 2000). Computed tomography has a lower sensitivity in detecting osseous metastases and an inferior diagnostic accuracy compared to MRI (Buhmann Kirchhoff et al, 2009). In fact, CT is less accurate in detecting paraspinal soft tissue, bone edema and bone metastases that may be missed if destruction is not present (Shah and Salzman, 2011). Therefore, CT has a rather complementary role in first line imaging of spinal metastases and owns priority only in those cases when the integrity and fine structure of the trabecular and cortical bone is a question, preoperative planning is required or when MRI is contraindicated. MRI is superior to CT in all other cases.

Metastatic lesions are most commonly focal or multifocal and the diffuse involvement of the vertebral bodies is less common. Focal abnormalities hypointense on T1 and hyperintense on T2 and short tau inversion recovery (STIR) sequences. In general metastases will enhance with contrast, although it is important to always acquire a non-contrast study for comparison. The diffuse marrow involvement can be difficult to assess, because a generally low signal intensity appearance can be misleading, giving the false impression of normal marrow. It is

helpful to compare the marrow's signal intensity to that of the discs and muscles. In adults it can be regarded as abnormal if the marrow has lower signal intensity than discs or muscles (Figure 2) (Long et al, 2010). Metastases tend to occur in the posterior part of the vertebral body, involving the pedicles. Most often metastases are destructive and can be expansive.

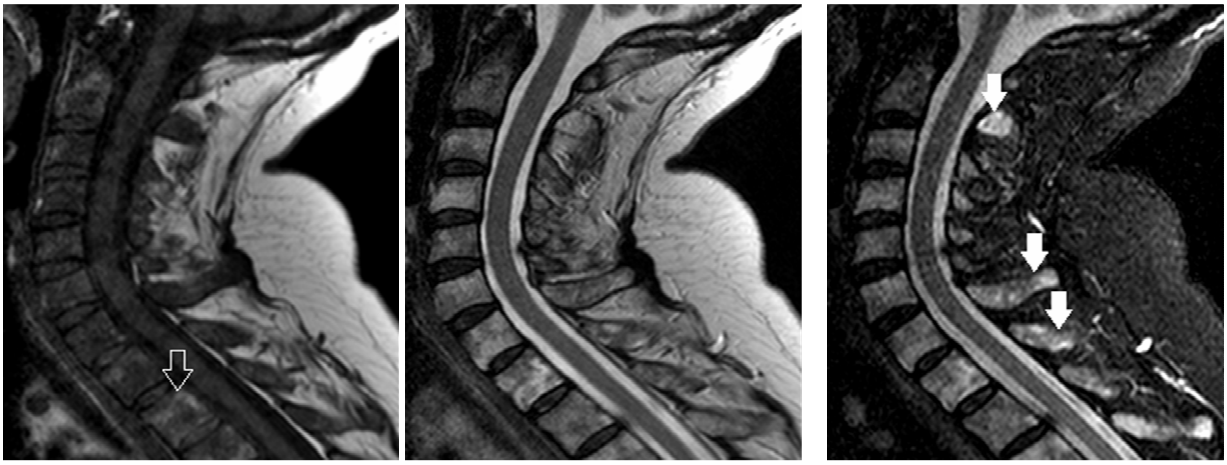

Figure 2. Diffuse metastatic involvement of the cervical and upper thoracic spine. The T1-weighted image (A) shows heterogeneous signal intensity in all vertebral bodies, with mostly isointense to hypointense signal accompanied by focal hyperintense areas (empty arrow) compared to intervertebral discs. On T2-weighted image (B) similar heterogeneity can be seen with hyperintense and isointense areas. On STIR sequence (C) diffuse hyperintense signal correlates with the T1 hypointensity, typical of metastatic disease of the bone marrow. The involvement of spinous processes is highly suspicious on T2 and becomes unquestionable on STIR (arrows). The focal hyperintensities on T1 are associated with fatty marrow and represented as hypointense signal on STIR.

In *osteolytic* metastases, the cancellous bone is replaced by tumor tissue and acceleration of bone resorption occurs due to an imbalance in metabolism. The focal disequilibrium in calcified elements will create the characteristic image of circumscribed translucency on radiographs and a generally low density area framed by intact, partly intact or sclerotic osseous components on CT. On MRI hypointense T1, hyperintnese T2 and STIR signals will represent the structural and biochemical (e.g. edema) changes in the bone marrow (Long et al, 2010). Posterior cortical and pedicle destruction is not infrequent and best visualized by CT. During the course

of antitumor therapy progressive sclerosis may be visible on follow up imaging, indicating positive response to therapy. Fluid levels may occur in lytic metastases (Jarraya et al, 2013) and might even mimic primary tumors (Colangeli et al., 2014). The term *osteoblastic* refers to the biologic behaviour of the lesions, but from the imaging point of view, *sclerotic* or *osteosclerotic* may sound more practical, as they reflect the imaging findings. Osteoblastic metastases are usually focal or mottled and in most cases are multifocal. Diffuse involvement of the vertebral body occurs occasionally. On MRI the lesions show T1 and T2 hypointensity. On T2 and STIR images a bright rim surrounding the sclerotic lesions may be depicted, reflecting bone marrow edema. This is known as the "halo" sign. Edematous signal can often be observed on STIR, expanding from the body to the pedicles, without a well-defined lesion on T1 or T2 sequences. The enhancement pattern in MRI may vary depending on the degree of sclerosis. On CT and plain film these lesions show high density resulting from excessive calcification. The epidural expansion of the tumor may create the "draped curtain sign" which can be depicted on axial MRI slices. (Figure 4)

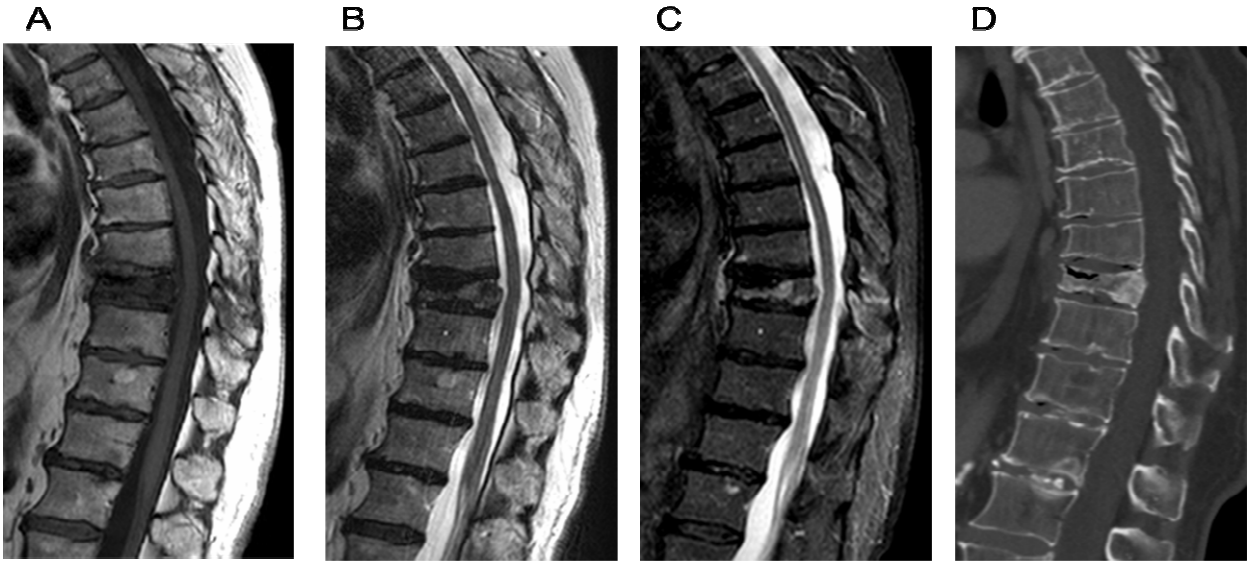

Figure 3. Compression fracture resulting from metastatic disease. T1 hypointense (A), T2 intermediate-hyperintense (B) and STIR hyperintense signal (C) is demonstrated in the compressed T9 vertebral body. The body shows a vertebral plana deformity. Posteriorly focal sclerotic changes can be observed on the sagittal reconstruction of CT scan (D).

Vertebral Compression Deformity

Vertebral compression deformity is frequent in elderly patients. The cause of this abnormality can be benign or malignant. Distinguishing between benign and pathological vertebral body compression fractures is usually possible on MR imaging. Chronic benign fractures typically have marrow signal intensity that is isointense with normal vertebrae on all sequences. In addition, there is no involvement of the posterior elements, absence of paravertebral or epidural mass and preservation of posterior cortex. Pathologic fractures show comparatively low signal intensity on T1- and high signal intensity on T2-weighted sequences (Figure 3) (Griffith et al, 2010). Pathologic compression fractures typically enhance with contrast; however, conventional MR techniques cannot always be used to differentiate benign from malignant lesions due to their similar appearances. For example, osteoporotic compression fracture can be confused with metastatic compression in the acute phase. Edema in an acute benign compression fracture replaces the normal marrow, resulting in hypointensity on T1-weighted images and hyperintensity on T2-weighted images. The vertebral body with benign fracture may enhance with contrast. These MR signal intensity characteristics are similar to those of metastases and cause ambiguity, especially when only a single lesion is present. Pathologic fractures are often multiple; other key features of pathologic compression fractures include loss of the posterior body height, pedicle involvement, epidural and paraspinal mass.

Diffusion weighted imaging (DWI) is emerging as a powerful clinical tool for directing the care of patients with cancer (Padhani et al, 2011). The basic biological premise for the use of DWI is the characteristic increased cellular content of malignant tissue, and increased water content. These features result in higher signal intensity of malignant disease on high b-value images with corresponding low apparent diffusion coefficient (ADC) values (Khoo et al, 2001). This is especially helpful in patients with neuroblastomas, leukemia, lymphoma rhabdomyosarcoma, Ewing sarcoma and metastatic Primitive Neuroectodernal tumors (PNET). Diffusion weighted imaging can also be a useful tool for distinguishing acute benign osteoporotic from malignant

vertebral compression fractures, resulting in low or iso-intense signal on DWI and high ADC values on ADC maps (Rumpel et al, 2013; Duvauferrier et al, 2013).

Whole body STIR has also been used to monitor disease progression in patients with lymphoma, multiple myeloma, metastatic PNET and neurofibromatosis (Fayad et al, 2013).

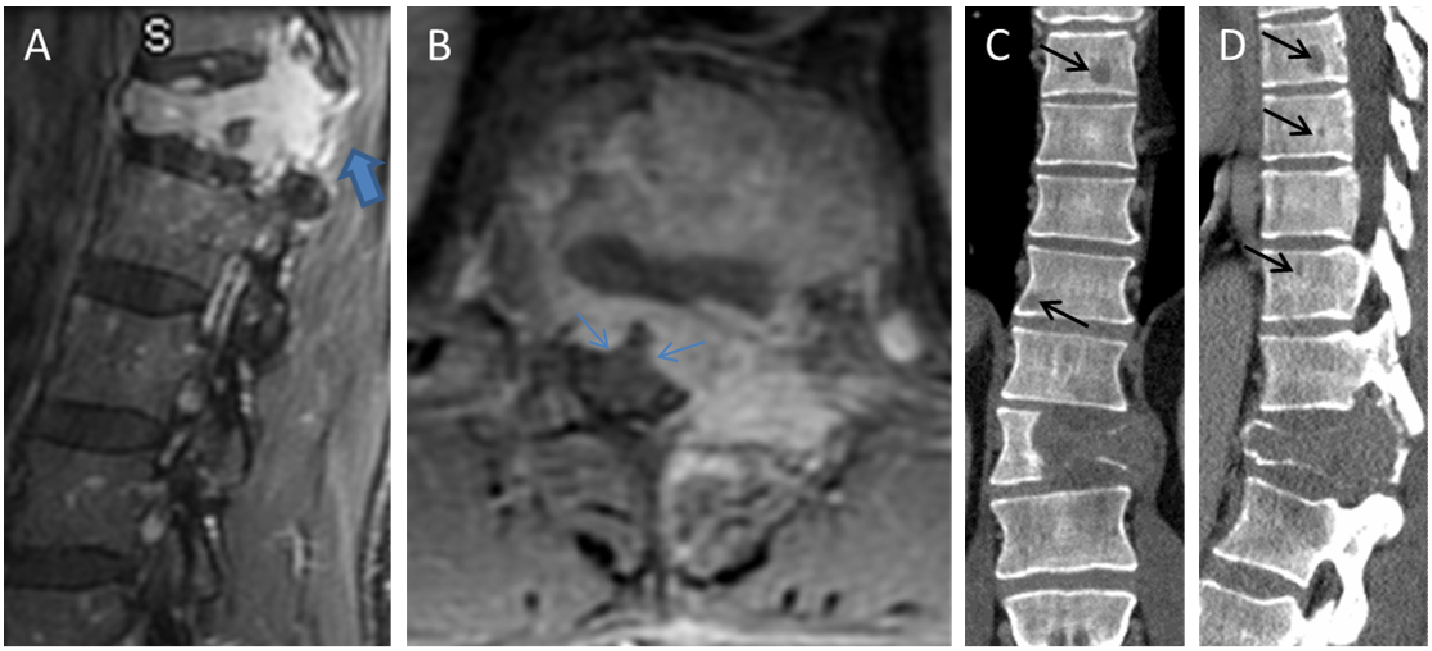

Figure 4. A 48 year-old male with multiple myeloma. Sagittal (A) and axial (B) contrast-enhanced T1-weighted scan with fat suppression show a large enhancing mass occupying the body of the T12 vertebra and extending into the spinal canal and into the pedicle on the left (arrows). The arrows on the axial image mark as the tumor invades the anterior epidural space bilaterally and compression on the thecal sac, creating the "draped curtain sign". Reformated CT in the coronal and sagittal plans (C and D) show the osteolytic nature of this tumor. This was thought to be a solitary plasmacytoma. Further imaging revealed "punched-out" osteolytic lesions (black arrows) characteristic of multiple myeloma.

PRIMARY TUMORS OF THE SPINE

Benign Primary Spine tumors

Hemangioma is the most common primary tumor of the spine, the incidence from autopsy studies is estimated to be 10% (Ropper et al., 2011). Histologically they consist of multiple small, thin-walled vessels interspersed with trabeculae and infiltrating the medullary cavity. Hemangiomas have a characteristic CT appearance with

polka-dot appearance on the axial images, which represent the cross section of the prominent vertical trabeculae. On MRI lesions show high signal intensity on T1 and T2 images, often with a heterogeneous structure, which may also contain flow-voids as signs of vascular elements. *Osteoid osteomas* occur in young adults and their most common symptom is a painful scoliosis that worsens at night (Theodorou et al., 2008). They usually arise from the posterior elements. Lumbar spine involvement is typical. On radiographs osteoid osteomas have the appearance of a lytic lesion surrounded by sclerotic rim. The same finding is present on CT scans. The sclerotic changes may affect the central area or *nidus*. On T1 images the nidus displays intermediate signal intensity and can have signal voids as a result of calcification. On T2 images the nidus appears as a low intensity area surrounded by high intensity rim representing edema. *Osteoblastomas* have a nonspecific MRI appearance, with T1 and T2 prolongation depending on the degree of matrix mineralization. Osteoblastomas have a reactive rim similar to osteoid osteomas, which can lead to overestimation of lesion (Chai and Cho, 2013).

Aneurysmal bone cysts (ABC) are expansile lesions containing blood-filled cysts separated by walls of bone (Long et al., 2010). The spine is effected in 12-30% of all ABC cases. On CT scans ballooning, lobulated cystic lesions can be found occasionally with fluid-fluid levels (Ropper et al., 2011). The latter is indicative of haemorrhage and may be more sensitively visualized by MRI (Figure 5). Signal changes, representing blood degradation products of different age can be appreciated. (Vidal and Murphey, 2007). *Giant cell tumor* (GCT) is a benign, locally aggressive tumor that accounts for approximately 4–5% of primary bone tumors. Most commonly, GCTs are found in long bones. CT and MRI may reveal an associated soft tissue component, and contrast administration may help to differentiate the bony and soft tissue elements. On MRI, they appear as low to intermediate signal intensity on T1- and T2-weighted imaging. GCT often causes the destruction of sacral foramina. *Osteochondroma* is an uncommon tumor, accounting for about 4% of solitary spinal tumors. Osteoschondromas seem to demonstrate distinct predilection for certain parts of the spine, specifically C2. It is often difficult to discover the lesion on radiograph or MRI images due to its small size and the continuity with

the bone it originates from. Thin slice CT scans may be needed to confirm the diagnosis (Vidal and Murphey, 2007).

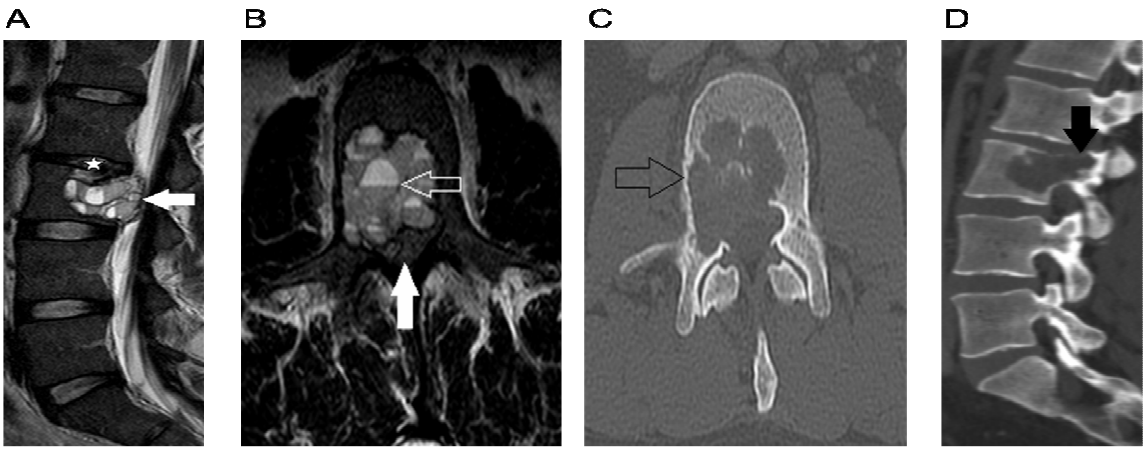

Figure 5. Aneurysmal bone cyst (ABC). Sagittal and axial T2-weighted images (A and B respectively) show a well-defined, multi-lobulated lesion in the L3 vertebral body. The lesion consists of several small cystic compartment which demonstrate sharply separated areas of T2 hyperintense and intermediate signal, representing fluid-fluid levels due to gravitational forces. This is best demonstrated on the axial T2 scan due to the supine position of the patient (white empty arrow). The lesion extends to the spinal canal and causes the compression of the dural sac (white arrows). CT scan with bone reconstruction (C) shows an almost complete replacement of osseous tissue by the lesion with only a thin layer of cortical bone remaining on the right side (black empty arrow). It also depicts the ballooning character of the lesion ad some sclerotic changes on the margins. The invasive nature of the ABC is also highlighted by the partial destruction of the upper endplate as displayed by the sagittal T2 scan (asterisk). On sagittal reconstruction of the CT scan (D) it is also clear that the lesion extends posteriorly into the pedicle (black arrow).

Malignant primary spine tumors

Chondrosarcoma is the second most common non-lymphoproliferative malignant tumor of the spine in adults (Rodallec et al., 2008). The mineralized matrix is best visualized by CT, and areas of calcification are represented as signal voids on MRI. The non-calcified tumor shows low attenuation on CT, low to intermediate signal intensity on T1 and high signal intensity on T2 images due to the water and hyaline content. Spinal *osteosarcomas* are the rarest tumors of the spine, accounting for 4% of all osteosarcomas and 5% of primary malignant spine tumors. Each level may be involved, but the thoracic and lumbar are most common. In the

majority of cases, the lesions arise from posterior elements. Osteosarcomas are osteoblastic tumors, hence their main imaging characteristics. The mineralized matrix of these tumors allows for detection by plain film or CT, occasionally creating the image of "ivory vertebra". MRI can assess the extent of the tumor, the soft tissue component and nerve root involvement, if present. On bone scintigraphy osteosarcomas show marked tracer uptake. *Ewing sarcoma* of the spine occurs in 5% of patients with Ewing's tumor, predominantly involving the sacrum, half of which have extraosseous soft tissue mass. 90% occur before the age of 20, although a second peak is observed at age 50. STIR is the most sensitive sequence. Ewing's sarcoma accounts for nearly 20% of spinal cord compression in children. *Neuroblastoma* is the most common cause of spinal cord compression in children less than 5 years of age. Typical imaging findings include T1W hypointensity with epidural or paraspinal mass, T2W hypointensity due to hypercellularity (Simon et al, 2012; Rossi et al, 2007)).

Chordoma accounts for 1–4% of all primary malignant bone tumors and is the most common non-lymphoproloferative primary malignant tumor of the osseous spine in adults (Vidal and Murphey, 2007, Rodallec et al., 2008). Chordomas are almost always located in the midline, the most common sites are the sacrum (50%) and the clivus (35%), followed by the cervical and thoracolumbar spine. CT aides in assessment of the extent of the tumor and distinguishes soft tissue from calcified areas (Atlas, 2009) (Figure 6). Imaging from MR reveals a destructive, lobulated mass that exhibits low to intermediate signal intensity on T1-weighted imaging and high signal intensity on T2 and STIR sequences. MRI is the best to evaluate the soft tissue and probable epidural component of the tumor. Chordomas display heterogeneous contrast enhancement with multiple septa and may invade the intervertebral disc space (Long et al, 2010).

Hematologic Malignancies of the spine

A *plasmacytoma* is a focal proliferation of malignant plasma cells. Plasmacytomas are thought to represent the early stage of multiple myeloma. Second lesion is found in 33% of cases presumed to be solitary plamocytoma. They tend to be located in the thoracic spine without predilection of anterior or posterior elements. In about two third of cases, a characteristic appearance is present with lytic and expansile replacement of cancellous and

partly intact, or even sclerotic cortical bone (Long et al., 2010). This may produce the image of a "minibrain" on axial CT images (Rodallec et al., 2008). In one-third of cases the image is less characteristic with a bubble like cystic appearance. Purely sclerotic plasmacytomas are rare. On MRI low T1 and variable or high T2 signal with varying degrees of contrast enhancement is demonstrated. *Multiple myeloma* is the most common primary neoplasm of bone (Long et al., 2010). Through the secretion of osteoclast-activating factors it causes excessive osteolysis resulting in multiple osteolytic lesions along the skeleton and skull. Conventional radiographs show the classic appearance of osteopenia with punched-out lesions, accompanied by compression fractures. Bone scintigraphy is not reliable for staging or monitoring. On MRI the pattern of multiple myeloma is characterized by numerous rounded foci of low T1 and high T2 and STIR signal, with mild to moderate enhancement. (Long et al, 2010). *Lymphoma* of the spine may present in the bone as primary disease or as metastases. 30% of systemic Non-Hodgkins lymphoma have skeletal involvement. In addition, epidural; leptomeningeal and intramedullary forms have been well described. T2WI and ADC show relative hypointensity due to the hypercellular nature of the disease ("blue cell tumor").

Primary tumors of the spine are summarized in Table 1.

		Location	MRI	CT	Other
Primary Benign	Hemangioma	Usually confined to vertebral body, but may extend to pedicle	T1 and T2 hyperintense; often heterogeneous with flow voids; STIR: different degrees of suppressed signal depending on fat content	White polka-dot appearance	Most common tumor of the spine- 10-12% 25-30% multiple Negative bone scan. Enhances intensely T1W hypointense-"aggressive" variant
	Osteoid osteoma	Posterior	Central nidus is	Osteolytic	Marked tracer uptake in nidus on technetium
		<2cm; typically lumbar spine; soft tissue mass may be present	and hypointense on T2; edematous rim on T2 and STIR; nidus may show calcifications (signal voids)	sclerotic rim	Cause of painful scoliosis in child or young adult Focal scoliosis concave on side of tumor Second decade
	Osteoblastoma	>1.5-2cm Neural arch Cervical most common	Similar to osteoid osteoma; T1 and T2 signals depend on degree of calcification	Well-circumscribed expansile	Scoliosis 50-60% Bone scan positive Variable enhancement Second and third decade
	Aneurysmal bone cyst	Neural arch extending into Vertebral body	Multiple cystic component; fluid-fluid levels due to bleeding and sedimentation; rim and septal enhancement	Balooning, osteolytic lesion with sclerotic rim	X-ray: lucent, expansile lesion Nocturnal back pain absent pedicle sign no malignant degereration
	Giant cell tumor	Most common in long bones; most frequent spinal location is sacrum	Low-intermediate signal; CE scan to assess soft tissue Heterogeneous enhancement	May reveal the destruction of sacral foramina	Locally aggressive Bone scan positive Lytic, expansile lesion Third decade
	Osteochondroma	Common in C spine (C2)	May miss a small tumor	Modality of choice	Spinous/transverse process Spinal lesions more common in males
Primary Malignant	Chondrosarcoma	Calcified and non-calcified part 5% in spine	Non-calcified part is hypointense or intermediate on T1 and hyperintense on T2; peripheral and septal enhancement	Best to visualize mineralized matrix	Low-grade, but third most common primary malignant bone tumor Bone scan positive Cortical disruption Fifth decade
	Osteosarcoma	thoracic and lumbar most common; arises in posterior elements	Soft tissue component T1-hypointense, T2 hypointense	Osteoblastic lesion; occasionally "ivory vertebra"	Bone scan: marked tracer uptake Metastases in lung, bone , liver Peak incidence in fourth decade Invades spinal canal Maybe seen in patients with Paget's disease
	Chordoma	Midline; most common is sacrum and clivus; discs usually involved	destructive lobulated mass; hypointense or intermediate on T1,; hyperintense on T2 and STIR; heterogeneous enhancement with septa	Bone destruction; soft tissue mass with amorphous calcification	90% local recurrence Enhance heterogeneously T2WI- very high signal with disc involvement Bones scan –normal or decreased uptake
	Neuroblastoma	Most common cause of cord compression in children < 5	T1W hypointensity with epidural or paraspinal mass; T2W hypointensity	Enhancing paraspinal mass with stippled calcification	bone scan positive Associated with opsomyoclonus (2-3%) "dumbbell" appearance
	Ewing-sarcoma	5% in spine Mostly sacrum; 50%	STIR most sensitive Moderate enhancement T1 hypointense, T2 intermediate /hyperintense	Tiny perforations of the cortex	20% of spinal cord compression in children Male-to female ratio is 2:1 Bone scan positive Fever , leukcytosis elevated sedimentation rate
Lymphoproliferative	Lymphoma	osseous, epidural, cord or leptomeningeal	Diffuse enhancement, epidural extension Whole body MRI with T1WI, STIR and DWI	Lytic, paraspinal mass	30% of systemic lymphoma have skeletal involvement Most are Non-Hodgkin's lymphoma Primary osseous lymphoma –good prognosis
	Plasmacytoma	Most often thoracic spine	T1 hypointensity; T2 signal varies; variable enhancement STIR hyperintense	In 2/3 of cases lytic expansile replacement of spongiosa	Poor prognostic factors are large size and M protein persistence after radiotherapy M:F 2 to 1, No/low level M-protein Bone scan- positive
	Multiple myeloma	Along the whole skeleton and the skull	Multiple rounded foci; T1 hypointense; T2 and STIR hyperintense	Multiple osteolytic lesions	X-ray: osteopenia with punched out lesions; bone scan not reliable, but PET is

INTRADURAL EXTRAMEDULLARY TUMORS

The most common intradural extramedullary lesions are schwannomas, meningiomas, and neurofibromas (Abul-Kasim,et al 2008). The range of tumors found in the intradural extramedullary space is few in comparison with bony or central cord tumors. Most of these masses originate from a systemic/congenital disorder such as the phakomatoses or are metastases from systemic cancers. The current standard diagnostic study for a spinal tumor is MR imaging (Setzer 2007). An MR image provides precise positioning on the extent of spinal cord compression, and further information about the spinal cord and tumor itself. The imaging protocol should include sagittal and axial T1-weighted and T2-weighted sequences including contrast-enhanced sagittal and axial T1-weighted sequences, and if needed, coronal images. The short-time inversion recovery (STIR) sequence is excellent for evaluating intramedullary cord lesions as well as marrow and soft tissue edema. Contrast-enhanced images are important to define the extent of the lesion and are useful in distinguishing associated cysts or syrinx from neoplastic involvement and are important in postoperative follow-up (Abul-Kasim,et al 2008; Bloomer, 2006).

Leptomeningeal Metastases

Leptomeningeal metastasis (LM) occurs by tumor cells infiltrating into the arachnoid and the pia mater (leptomeninges), causing focal or multifocal infiltration. This metastatic condition can be observed in solid, hematologic, and primary brain tumors. (Bruna, Simo and Velasco,2009). LM is diagnosed in 4% to 15% of patients with solid tumors. The most involved neoplasms are breast (12-35%), lung cancer (10-26%), melanoma (5-25%), gastrointestinal cancer (4-14%), and cancers of unknown primary origin.(1-7%) (Bruna et al 2009; Clarke et al, 2010; Kesarti and Batchelor 2003; Le Rhun et al, 2013). However, LM is likely underestimated considering that autopsy studies reveal a frequency of LM is 19% to 40% in patients with cancer. Common primary central nervous system (CNS) tumors that may spread to the leptomeninges, so-called “drop Metastasis” are maliganant astrocytomas, ependymomas, or medulloblastomas. LM from CNS neoplasms occurs in younger patients, whereas metastases from lung or breast carcinomas occur in older

patients. Abnormalities of the standard cerebral spinal fluid (CSF) analysis are observed in more than 90% of the cases of LM. These abnormalities are nonspecific and include increased opening pressure (>200 millimeter of water) in 46%, increased leukocytes (>4/mm^3) in 57%, elevated protein (>50 milligram per deciliter) in 76%, and decreased glucose (<60 mg/dl) in 54% (Le Rhun et al, 2013). The gold standard is finding neoplastic cells on CSF examination. While highly specific, the first lumbar puncture has low sensitivity with a yield estimated at 45-55%, which increases to 80-90% with a second lumbar puncture (LP).

Imaging

LM involves the entire neuroaxis, and therefore, imaging of the entire CNS is required. MRI with gadolinium enhancement is the neuroimaging modality of choice to evaluate individuals with LM (Bruna et al, 2012; Le Rhun et al, 2013). MRI should be obtained before LP to rule out to rule out the presence of parenchymal metastases and to estimate the subsequent risk of cerebral herniation following the procedure (Bruna et al, 2009). It also provides essential support in making a reliable diagnosis of LM in the appropriate clinical setting when CSF is negative (Bruna et al, 2012) The sensitivity of MRI varies from 20% to 91% (Clarke et al, 2010; de Azevedo et al, 2011; Gauthier et al, 2010; Rudnicka et al, 2007). A normal MRI following a negative CSF does not exclude LM. Nonetheless, in cases with a typical clinical presentation, abnormal MRI alone is adequate to establish the diagnosis of LM and treatment should be initiated.

The spine is best evaluated with sagittal T1-weighted sequences with and without contrast and sagittal fat suppression T2-weighted sequences, combined with axial T1-weighted images with contrast. Contrast enhanced T1-weighted and fluid attenuated inversion recovery (FLAIR) sequences are also sensitive to detect LM (Dietemann et al, 2005). The most frequent MRI findings are subarachnoid and parenchymal enhancing nodules, diffuse or focal pial enhancement, and nerve root enhancement (Figure 6) (Le Rhunn et al, 2013).

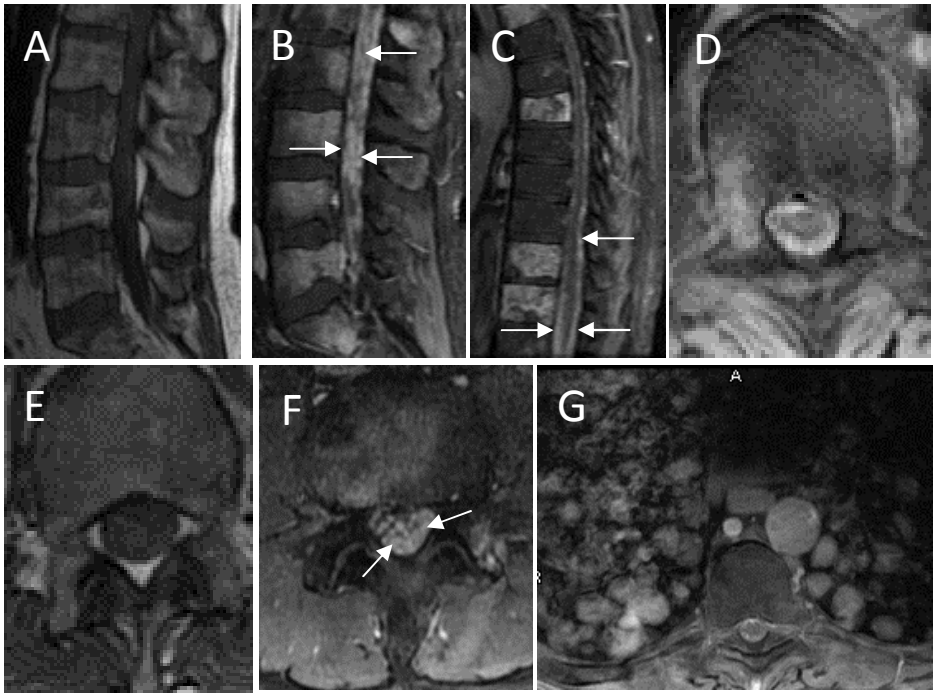

Figure 6. 50-year old male with metastatic melanoma. Sagittal and axial T1-weighted post gadolinium images show diffuse enhancement of the leptomeninges, or so called "sugar coating" or zuckerguss, within the thoracic spine (C and D), as well as the nerve roots of the cauda equine (B and F). These images are compared to sagittal and axial pre-contrast T1- weighted images (A and E) Also notice multiple enhancing vertebrae (B and C) pulmonary nodules consistent with metastatic disease (G).

Meningiomas

More than 95% of meningiomas are benign slow growing tumors (WHO grade I) (Abul-Kasim et al, 2008; Bloomer et al, 2006). They are the second most common intraspinal tumors and are second only to nerve sheath tumors. Spinal meningiomas represent 12% of all meningiomas (Setzer et al, 2007). Most meningiomas arise from arachnoid meningothelial ("cap") cells near the dorsal root ganglion (Bloomer et al, 2006; Arnautovic et al, 2009). Most (90%) of spinal meningiomas are intradural, 5% are both intradural and extradural in a dumb-bell fashion, and 5% are only extradural. There is a female predominance of 4:1 to 10:1(Bloomer et al, 2006), usually presenting after the fourth decade. The most common location is the thoracic region (80%), 15% in the cervical, followed by 5% in the lumbar spine. Meningiomas are often located posterolaterally in the thoracic region and anteriorly in the cervical region. Multiple meningiomas are rare except in patients with neurofibromatosis type 2. Spinal meningiomas are usually benign, slow growing tumors with a long clinical history until a diagnosis is made. The mean duration of symptoms is 12-24 months (Setzer et al, 2007). Clinical

symptoms are typically dependent on the tumor location with respect to the spinal cord or nerve roots, the rate of tumor growth, and the extent of spinal cord compression. The introduction and routine use of MR imaging has shortened the time to diagnosis of the spinal meningioma and therefore has improved outcomes (Setzer et al, 2007; Klekamp et al, 1999).

Imaging

Meningiomas are usually discrete lesions, with a broad dural base. The dural tail and calcification may be seen, but they are less common than in the intracranial meningiomas. Spinal meningiomas are typically iso-to hypointense on T1-weighted images and isointense to spinal cord on T2-weighted images. Calcification occurs in less than 5% of patients, and results in low T1 and low T2 signal intensity. In general, meningiomas demonstrate strong homogeneous enhancement after gadolinium administration, except for calcified areas (Figure 7) (Abul-Kasim et al, 2008; Bloomer et al, 2006; Liu et al, 2009). Meningiomas cause compression and displacement of the spinal cord. Signal changes in the spinal cord secondary to compression may be rarely seen (Abul-Kasim et al, 2008). The main differential diagnosis of spinal meningiomas includes intradural extramedullary. Meningiomas enhance moderately and almost always in a diffuse fashion, whereas schwannomas enhance very strongly, most of the time with an irregular appearance. Schwannomas tend to exhibit a ring-like enhancement. The dural tail sign is helpful in the diagnosis of spinal meningioma but is considered nonspecific. Most schwannomas are hyperintense on T2-weighted images and their signal is heterogeneous compared with that of meningiomas (De Verdelhan et al, 2005).

Figure 7. A 66 year old female with progressive onset of weakness, spasticity, and paresthesias in her lower extremities. At the level of T8, there is a large extraaxial mass lesion within the posterior spinal canal severely compressing the spinal cord best demonstrated in figures D & E (arrow heads outline the spinal cord compression). This mass is isointense on T1WI (fig A), and on T2WI (B & E). There is hypointensity in the center of the lesion on all sequences representing calcification (A-C, arrows). There is homogeneous enhancement except in the area of calcification (C & D).

Peripheral Nerve Sheath Tumors

Nerve sheath tumors account for 30% of intradural/extramedullary tumors and are histologically either schwannomas or neurofibromas (NF). The peak incidence is in the fourth and fifth decade. Symptoms may be present for more than two years before diagnosis as there is usually little functional impairment. Schwannomas (neurilemomas) are composed of Schwann cells and produce an eccentric enlargement of the involved nerve root. Neurofibromas are a mixture of Schwann cells and fibroblasts with abundant collagen fibers and cause diffuse enlargement of the nerve root. Unlike meningiomas, which occur more often in females, there is no sex predilection (Bloomer et al, 2006). Schwannomas, which are considered benign WHO grade 1 tumors, are the most common intradural extramedullary spinal lesions, followed by meningiomas (Abul-Kasim et al, 2008). Schwannomas are more commonly seen in adults and often associated with neurofibromatosis II (NF-II). Multiple schwannomas in the absence of other features of NF-II are seen in schwannomatosis (MacCollin et al, 2005). In 90% of cases, neurofibromas are solitary tumors. The age of onset is 20-30 years. Multiple tumors are seen in people with NF I. Seventy percent are intradural/extramedullary in location, 15% are purely extradural,

and 15% have both intradural and extradural components (“dumb-bell” lesions). Less than 1% are intramedullary (Gottfried et al, 2003).

Imaging

Schwannomas and neurofibromas are often indistinguishable radiographically. Plain films and CT may demonstrate foraminal enlargement, pedicular erosion, posterior vertebral scalloping, thinned lamina, or a paravertebral soft tissue mass.

Schwannomas are infrequently associated with hemorrhage, cyst formation, and fatty degeneration. These findings are rare in neurofibromas. Neurofibromas encase the nerve roots in a fusiform manner, whereas schwannomas commonly displace the nerve roots due to their asymmetric growth (Abul-Kasim et al, 2008; Bloomer et al, 2006). Both tumors are iso-to hypointense on T1-weighted imaging, and markedly hyperintense on T2-weighted sequences, including STIR. However, schwannomas may have mixed signal on T2-weighted imaging (Figure 8) A hyperintense rim and central area of low signal resulting in a “target sign” may be seen in neurofibromas and occasionally also in schwannomas (Figure 9). The low T2 signal intensity is due to hemorrhage, collagen, and densely packed Schwann cells (Bloomer et al, 2006). Following administration of gadolinium, intense and homogenous enhancement is seen. Some neurofibromas show only peripheral enhancement (Abul-Kasim et al, 2008; Beall et al, 2007; Soderlund et al, 2012; Aska and Amautovic 2014).

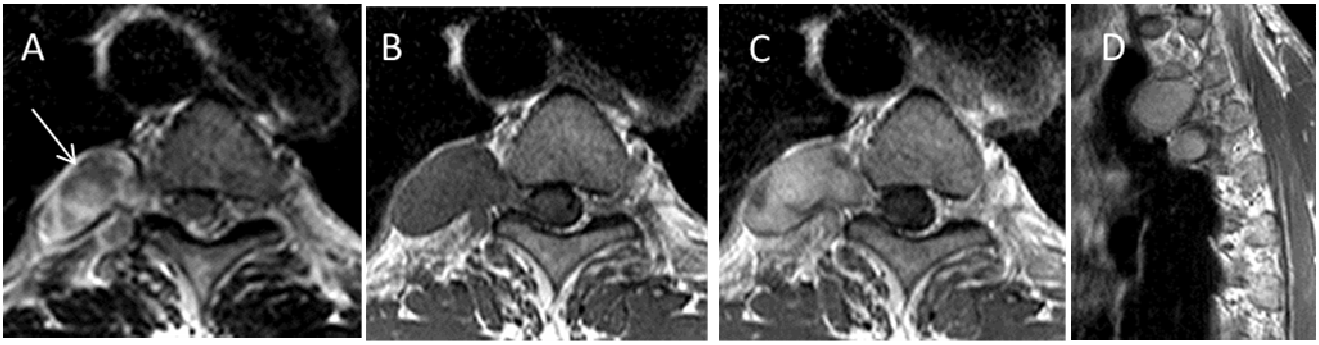

Figure 8. A 49 year-old male with NF-II, with a history of bilateral vestibular schwannomas, as well as multilevel schwannomas in the spine. The above images demonstrate a lobulated mass exiting the T4-5 neuroforamen on the right. It appears heterogeneous on T2WI (A), isointense to cord on T1WI (B), and enhances fairly homogeneously with contrast (C and D).

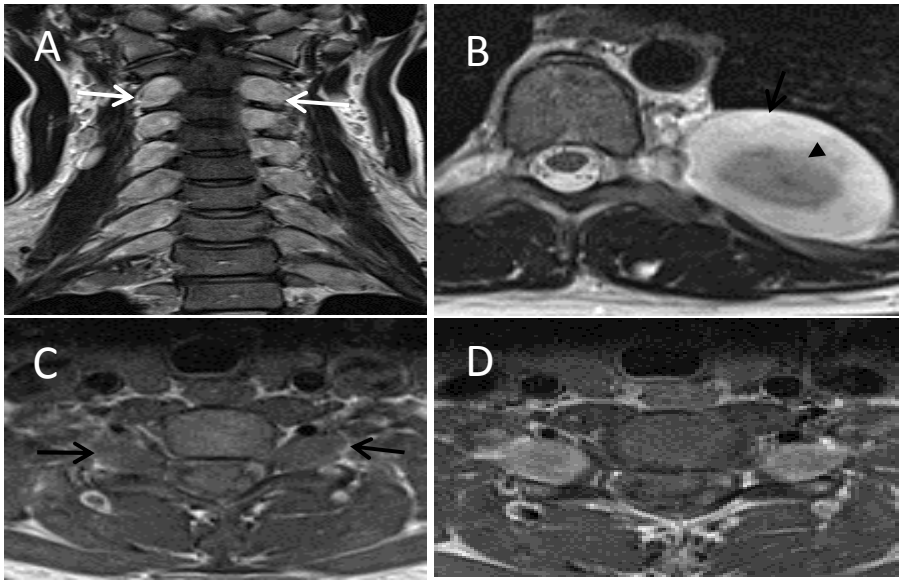

Figure 9. A 25 year-old female with a history of neurofibromatosis 1. The coronal image (A) shows multilevel T2 hyperintense fusiform masses exiting the neuroforamen (arrows). On the axial T2WI (B), there is a hyperintense rim (arrow) and central area of low signal (arrow head) resulting in a "target sign". They appear isointense on the T1WI (C, arrows) and enhance homogeneously following gadolinium (D).

The differential diagnosis of intradural extramedullary tumors also includes cysts and cyst-like lesions such *as arachnoid cyst, perineural cyst, epidermoid, dermoid cysts, and neuroenteric cyst* (Abdul-Kasim K. et al, 2008). Arachnoid cysts, epidermoid, and neuroenteric cysts are hypointense on T1-weighted MR images, similar to cerebral spinal fluid (CSF) and usually hyperintense on T2-weighted images, again similar to CSF. Dermoid tumors may be hyperintense on T1-weighted images due to the presence of fatty secretions of sebaceous glands and cholesterol. Signal intensity of both epidermoid and dermoid cysts may be homogeneous or heterogeneous.

The apparent diffusion coefficient of arachnoid cysts is similar to that of CSF. Epidermoid cysts and sometimes dermoid cysts have restricted ADC in comparison to CSF because of the squamous epithelial cells in the cyst. Epidermoid and dermoid cysts may have mild ring enhancement following contrast (van Aalst J et al 2009)

INTRAMEDULLARY SPINE TUMORS

Intramedullary spinal tumors account for 5 to 10% of all spinal tumors in adults and approximately 35% in children. About 90% of the tumors of the sp+inal cord are glial tumors of which the vast majority of these neoplasms are ependymomas and astrocytomas. Ependymomas represent about 60% and astrocytomas 30% (Duong et al, 2012). Of the remaining 10%, hemangiomablastomas account for 2-8% (Lonser et al, 2003) and 2% are intramedullary metastases (Vassiliou et al, 2012). Intramedullary tumors are more common in children, with extramedullary tumors being more common in adults. The intracranial/spinal ratio of astrocytomas is approximately 10:1, whereas the intracranial/spinal ratio of ependymomas can range from 3:1 to 2:1 depending on the specific histological variant (Duong et al, 2012). The distribution of spinal cord tumors is directly related to the length of the cord; thoracic cord has the most (50-55%), lumbarsacral is second (25-30%) and the cervical spine the least (15-25%) (Lonser et al, 2003).

Ependymoma

Half of all ependymomas are located below the foramen magnum and involve either the spinal cord (55%) or the cauda equina region (45%). The mean age of presentation is around 40 years and there is slight male predominance. Intramedullary ependymomas have a predilection for the cervical spinal cord such that 67% percent of tumors arise from or extend into this region. Ependymomas of the cord are typically solitary tumors that arise from the ependymal lining of the central canal causing a diffuse enlargement of the cord over several levels and the associated syrinx in 50% of the cases. Spinal cord ependymomas have only a slight tendency to

infiltrate the adjacent neural tissue and have a delicate capsule forming a plane of cleavage to separate tumor from spinal cord. The World Health Organization (WHO) recognizes five histological variants of ependymoma, including the cellular, papillary, epithelial, and tanycytic and myxopapillary subtypes. Ependymomas are also commonly divided into typical, WHO grade II, or anaplastic WHO grade III varieties. In addition, two low-grade (WHO grade I) forms, myxopapillary ependymoma and subependymoma have also been recognized. . Myxopapillary ependymomas of the filum terminale is a histologic variant accounting for about 13% of all ependymomas, but more than 80% of all ependymomas that are located in the conus medullaris and filum terminale.

MRI has reduced the duration from symptom onset to diagnosis from 24 to 36 months to 14 months and as a consequence, the incidence of weakness and sphincter involvement has decreased. The most common complaint (95%) at the time of diagnosis is back pain. Most patients have dysesthesias without sensory loss. This is attributed to the location of spinal ependymomas around the central canal; the symmetric expansion of the central canal causes an interruption of the crossing spinolthalamic tracts (central cord syndrome). When pain and numbness are in a radicular pattern involving the legs, the underlying tumors usually are myxopapillary ependymoma predominantly involving the cauda equina. Spinal ependymomas also have a tendency of causing micro hemorrhages and delaying diagnosis may lead to superficial hemosiderosis with involvement of the caudal cranial nerves. Unexplained superficial hemosiderosis seen on a cranial MRI should prompt a spinal investigation with MRI for the exclusion of spinal ependymoma. (Figure 10)

The association between neurofibromatosis II (NF-II) and spinal ependymoma is well known. This is an autosomal dominant disease caused by mutation of the merlin or schwannomin gene or chromosome 22. NF-II has been described as a Multiple Inherited Schwannomas, Meningioma and Ependymoma (MISME). The incidence of polar and tumoral cysts that are seen rostrocaudal to the tumor occurred in 50 to 90% of cases. On T1-weighted images cellular ependymomas tend to be isointense or slightly hyperintense to the spinal cord and

on T2-weighted images they appear to be hyperintense. Hemosiderin is seen as an area of hypointensity or so-called *cap sign,* this may occur in 20 to 64% of cord ependymomas. STIR sequence shows hyperintensity, while 80% of these cases on TWI enhance homogeneously with contrast. Minimal or no enhancement is actually relatively rare. Diffusion tensor imaging (DTI) may show the tumor displace the fiber tracts rather than interrupt them (Mechtler and Nandigam 2013).

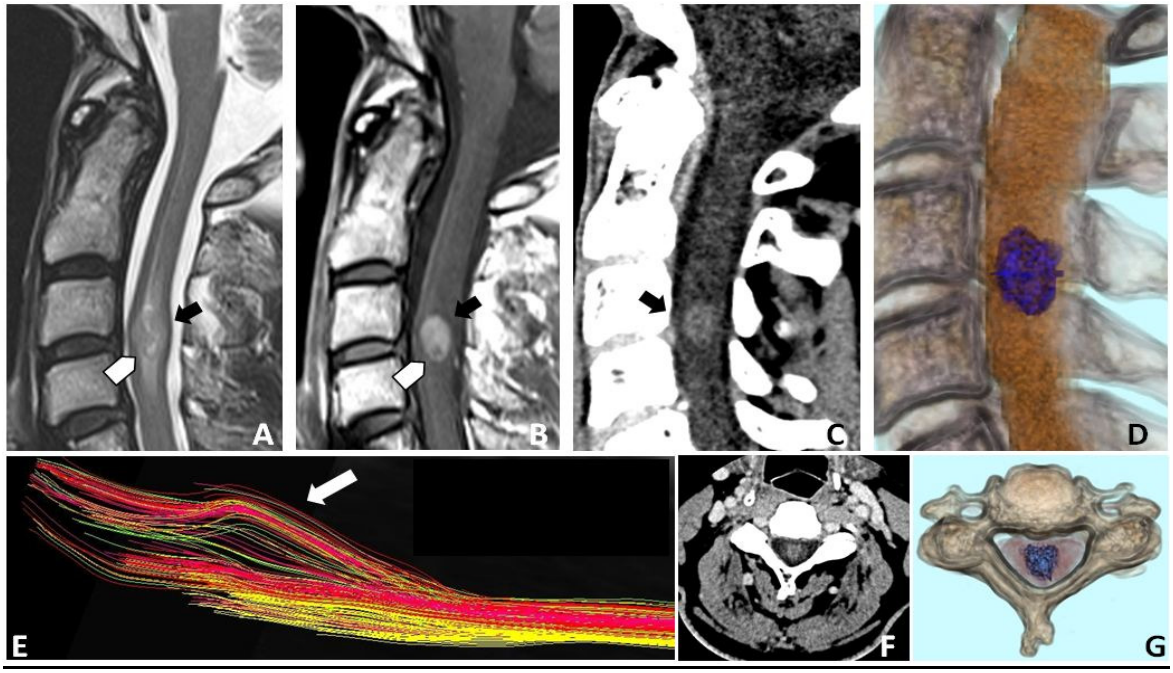

Figure 10. Patient is a 55 year old male who presented with progressive one year history of shawl-like dissociated sensory loss in the upper extremities as well as weakness, typical of a central cord syndrome. (A) T2W sagittal image shows a central cord mass (black arrow) with mild edema, with a rostral and a caudal (white arrow head) small polar cysts. On T1W sagittal with contrast, there is diffuse tumor enhancement. The polar cyst (white arrow head) does not enhance with contrast. Diffusion tensor imaging /tractography (E) confirms the non-infiltrative nature of this mass with fibers being displaced (white arrow). Post contrast images obtained on a 320-slice CT (C, F) and 3-D reconstruction in the sagittal (D)and axial (G)planes elaborates the bony structures surrounding this well demarcated enhancing ovoid (blue) spinal cord mass that was consistent with a cellular ependymoma.

Myxopapillary ependymoma of the conus medullaris and filum terminale is a relatively common spinal intradural neoplasm and found predominantly in children and young adults, although they may have to be observed at an older age. There is a slight male predominance. They appear as isointense/hypointense masses

on T1-weighted images and as hyperintense masses on T2-weighted images. They tend to be extramedullary and present as a cauda equine syndrome. They usually span 2 to 4 vertebral segments and they fill the entire lumbar sacral thecal sac. There may be posterior vertebral scalloping, as well as intravertebral foraminal widening. At times onT1 and T2-weighted images they may be hyperintense due to accumulation of mucin. On T2-weighted images they may also be hypointense due to tumor margin consistent with hemosiderin. STIR sequences tend to be hyperintense and the contrast enhancement is usually avid. The complete CNS axis must be imaged because of the potential for leptomeningeal seeding. Myxopapillary ependymomas are the most common subtype of ependymomas that hemorrhage. (Figure 11)

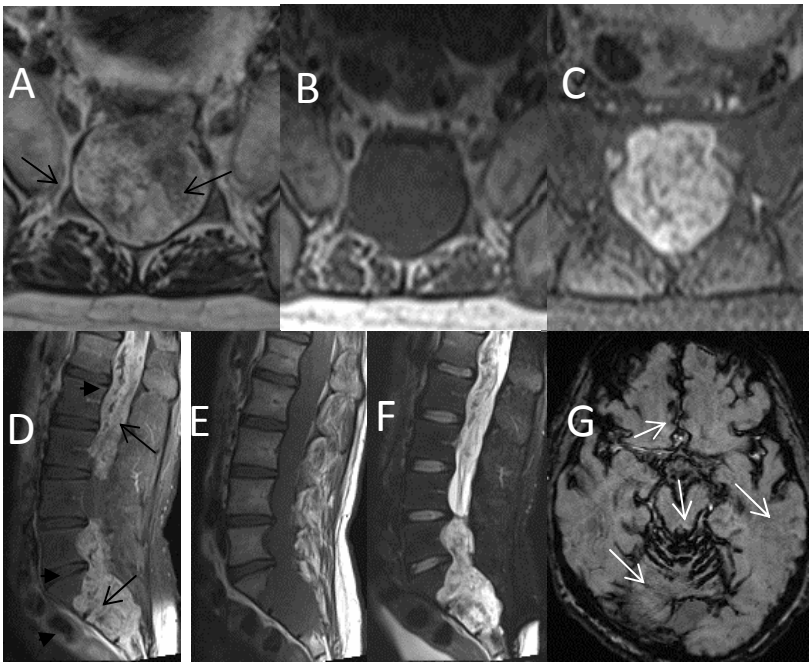

Figure 11 . A 27 year-old male with chronic bilateral lower extremity pain and numbness who has biopsy proven myxopapillary ependymoma. T2WI (A and D, arrows) shows hyperintense mass in the lumbosacral region causing scalloping of the posterior vertebrae and sacrum (arrow heads). The lesions appear isointense on T1WI (B and E), and strongly enhance with contrast C and F). SWI sequences of the brain (G) shows hypointensity ining the leptomeningeal surfaces of the brain (arrows) consistent with chronic hemosiderosis due to "cryptogenic" subarachnoid hemorrhage from the spinal tumor.

Astrocytoma

Intramedullary spinal astrocytomas account for 3 to 4% of all CNS astrocytomas. In adults they comprise 30 to 35% of all intramedullary spinal cord tumors, while in children they tend to be more common, comprising 90%

of all primary spinal cord tumors in patients less than 10 years of age and up to 60% of primary spinal cord tumors in adolescents. Gender distribution between male and female patients is fairly even. In adults the average age of onset is 29 years, a presentation that is earlier than that of ependymomas. The tumor arises in the cervical spinal cord in approximately 60% of patients. The tumor spanning the entire spinal cord, known as holocord tumors can occur, but are very rare. Histologically, gliomas can be differentiated as pilocytic (WHO grade I), fibrillary (WHO grade II), anaplastic (WHO grade III) and glioblastoma multiforme (WHO grade IV). Pilocytic astrocytomas tend to displace rather than infiltrate the cord. Statistically 89% of astrocytomas are low grade either fibrillary or pilocytic, 10 to 15% are high grade mostly anaplastic, while glioblastoma multiforme occurs in 0.2-1.5% of all cord astrocytomas. In general, astrocytomas cause asymmetric enlargement of the cord. The incidents of primary spinal cord astrocytomas are reported to be at 2.5 per 100,000 per year, being 10 fold less than primary astrocytomas of the brain. The clinical features of the spinal cord astrocytoma are initially localized low back pain and progressive weakness. Astrocyotomas have an affinity to white matter tracts which topographically are peripheral in the spinal cord. Hence the asymmetry that is characteristic of these tumors. Unlike ependymomas paresthesias are more common than dysesthesias (Mechtler and Nandigam, 2013).

In general astrocytomas are T1 hypointense/isointense in contrast to T2-weighted, which are hyperintense. Blood products occur in the minority of cases. Unlike most intracranial low grade astrocytomas, spinal 70-80% of astrocytomas enhance with gadolinium. (Seo et al, 2010). MRI shows a patchy nonhomogeneous pattern of enhancement consistent with diffusely fluctuating tumor. With contrast there is enhancement, this usually is mild to moderate. Contrast enhancement does not predict tumor grade or behavior, especially in pilocytic astrocytomas. Axial MRI images show an asymmetric expansion of the cord (Figure 13).

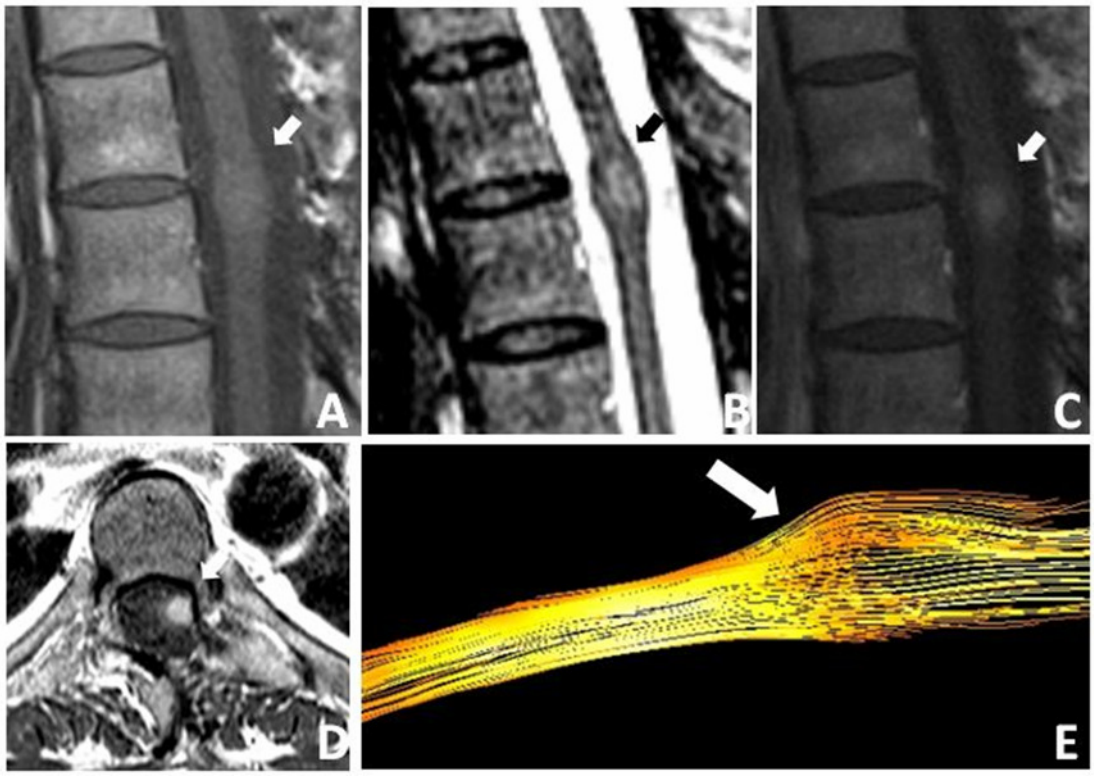

Figure 12. A 48 year old male with vague back pain and normal exam was operated on 9 years ago for an intramedullary mass. T1W non-contrast (A) and T2W sagittal images (B) show a focal asymmetric enlargement of the left cord that enhances homogenously) on T1W sagittal (C) and axial (D) contrast images. The images and clinical history is consistent with a pilocytic astrocytoma. 3 Tesla MRI diffusion tractography confirms typical findings in a non-infiltrative astrocytoma with fanning of the fibers around the tumor. FDG PET (not shown) showed hypermetabolism of the tumor which is also characteristic of pilocytic astrocytomas, despite being WHO grade I. Patient continues to be neurologically intact and asymptomatic and has not had any adjuvant treatment.

Hemagioblastoma

These are benign, WHO grade 1 tumors. The annual incidence is about 0.02/100,000 people. They comprise about 2 to 8% of all intramedullary spinal cord tumors. The cell of origin is uncertain, likely VEGF secreting cells (Harrop et al, 2009) of undifferentiated mesenchymal origin (Duong et al 2012). They can occur either sporadically, or associated with von Hippel-Lindau disease (25%). Mutations on the short arm of chromosome 3p25 are seen in VHL patients with hemagioblastomas (Lonser et al, 2003). Cervical and thoracic segments are

commonly involved, with a predilection for dorsolateral cord surface. The tumor can be single or multiple and tend to be smaller than 10 mm in diameter in patients with von Hippel-Lindau disease (Vassiliou et al, 2012). With sporadic spinal hemangioblastomas, the tumors can get bigger up to 6 cm in diameter. Grossly, they are well demarcated with a capsule and a characteristic abnormally dilated tortuous vessels on the surface. These tumors are isointense on T1-weighted images, and hyper intense on T2 weighted images (Vassiliou et al, 2012) (Figure 13). They may have mixed heterogenicity if intralesional hemorrhage is present. The contrast enhancement is usually homogenous, avid and well demarcated, with superficial heterogeneous enhancement within the flow voids. The surrounding vasogenic edema is mild. The flow voids are more common in tumors greater than 15 mm in size. Because of presence of dilated vessels, these tumors are often mistaken for a vascular malformation. The presence of syrinx, commonly seen in 30-60% (Vassiliou et al, 2012; Tihan et al 2006) on patients with hemagioblastoma, may help with the differentiation, which is uncommon with a vascular malformation. Spinal angiography to demonstrate enlarged feeding arteries, intense nodular stains, and early draining. The prognosis in general is usually excellent, although the tumor recurrence is common in patients with von Hippel-Lindau disease

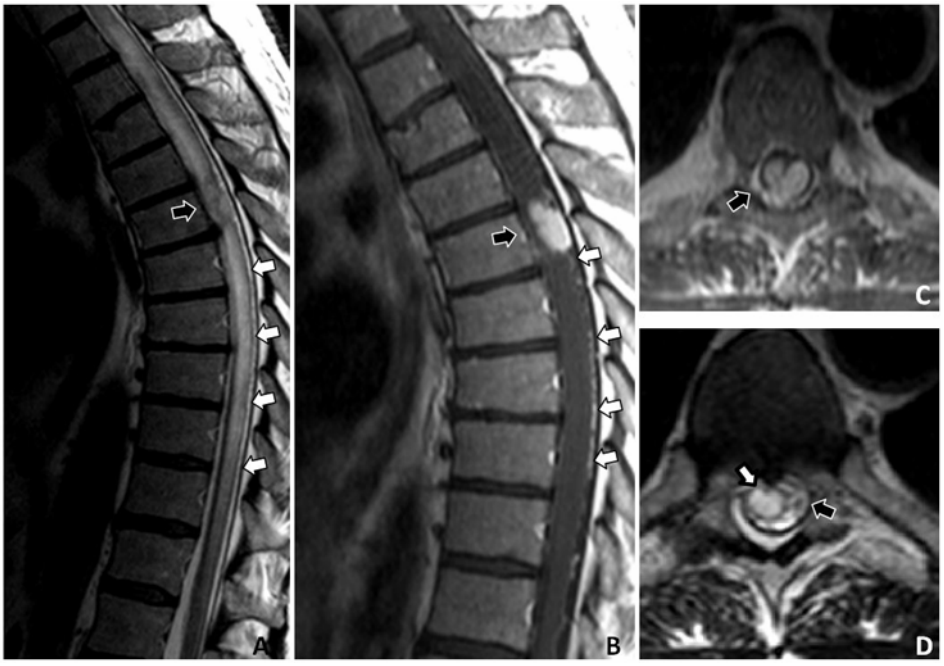

Figure 13. A 58 year old HIV male diabetic presents with left sided numbness, left partial foot drop and left upper abdominal pain progressing over a period of 6 months. A T2W sagittal image (A) show a heterogenous mass at T-6 (arrow) associated with extensive cord edema. Arrow heads show a hypointense linear structure consistent with a vessel posterior to the cord. On the contrast sagittal T1W image (B) an enhancing intramedullary bilobulated mass is seen. Furthermore, an enhancing engorged vessel is seen posterior and caudal to tumor (white arrow). Axial T1W contrast (C) shows an interesting bilobulated intra and extra medullary "snowman" appearance. T2W axial (D) hyperintensity (white arrow) is consistent with extensive holocord edema that resolved after surgery. The black arrow is a signal void from an abnormal vessel. Pathology was consistent with a hemangioblastoma.

Intramedullary Metastasis

Intramedullary spinal cord metastasis (ISCM) accounts for only 2% of all intramedullary spinal cord neoplasms (Kalaycki et al, 2004). The primary cancers responsible ISCM are lung (49%), breast (15%), lymphoma (9%), colorectal (7%), head and neck (6%), renal (6%) and melanoma (5%) (Wilson et al, 2012). There is a relative tendency for small cell lung carcinoma to metastasize to the spinal cord. ISCM is a relatively a rare sequela of systemic cancer with arguably the worst prognosis of all intramedullary spinal cord tumors. It is diagnosed in less than 1% of systemic cancer patients. ISCM are thought to be arterially disseminated, a notion that is supported by the fact that 55% of patients have systemic metastases and 41% have brain metastases (Schijns et al, 2000). The thoracic cord is the most commonly affected segment (57%). Nearly all lesions enhance, are well

circumscribed and solitary (Ryyken et al, 2013). (Figure 14) The edema is extensive and out of proportion to the size of the tumor.

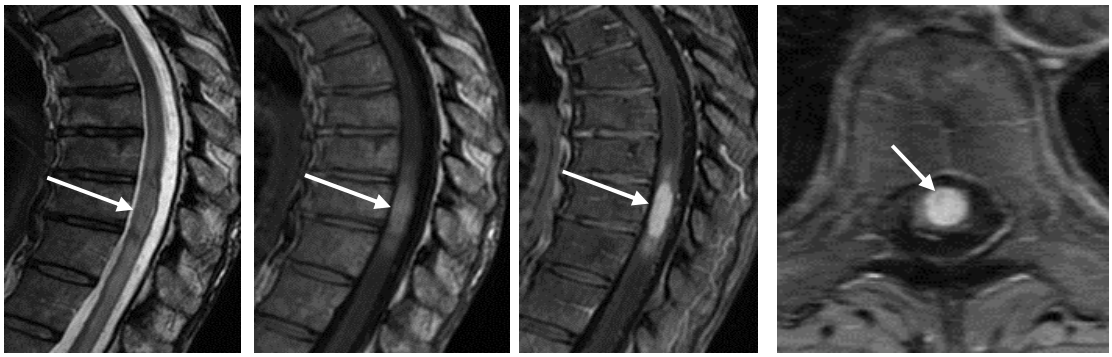

Figure 14. A58 year-old female who has a history of metastatic melanoma. MR images above show an intramedullary lesion at the level of T9 (arrows) with surrounding edema. The lesion is iso- to hypointense on T2WI (A), and hyperintense on T1WI (B) reflecting the tendency of melanoma to hemorrhage as well as the melanin in these lesions. Note the intense enhancement following contrast (C and D).

CONCLUSION

Routine MRI sequences have superiority in imaging of the bone marrow, the spinal cord and soft tissue making MRI the method of choice in spine tumors. 3T has become the de facto standard for neuroimaging of the spine (Fritz 2014). The major advantage of the 3T MRI is improved quality of high-end imaging, such as DWI, diffuse tensor imaging (DTI), perfusion weighted imaging (PWI), SWI, and MR spectroscopy (Vertinsky et al 2007). DWI and ADC may be markers for hypercellularity, especially in tumors of the spinal cord. DTI has the potential to help differentiate destructive intramedullary tumors from tumors that displace normal tissue, which can, in turn, decrease surgical morbidity. PWI can measure the degree of tumor angiogenesis and capillary permeability. SWI can increase the visibility of hemorrhagic, calcified, and vascular tumors (Wang et al, 2011). MRS is a noninvasive imaging technique that offers metabolic information on spine tumor biology that is not available from anatomic imaging, which may reflect the tumor grade and improve the differential diagnosis (Marliani et al 2007). The use of intraoperative MRI has led to advances in the extent of tumor resection. Neuroimaging is entering an exciting new era in which we can ask and expect to answer sophisticated questions

concerning spine tumors. The ultimate success of spine surgery will depend on the incorporation of anatomic and functional imaging with high-field MRI to diagnose patients sooner and more accurately, when patients' performance status is minimally affected. (Duprez et al 2008; Mechtler and Nandigam 2013).

Bibliography

Abdulazim A, Backhaus M, Stienen MN, et al (2011). Intramedullary spinal cord metastasis and multiple brain metastases from urothelial carcinoma. J Clin Neurosc,: Official journal of the Neurosurgical Society of Australasia 18:1405-7.

Abul-Kasim K, Thurnher MM, McKeever P, et al (2008). Intradural spinal tumors: current classification and MRI features. Neuroradiology. 50(4): 301-14.

Aguilera DG, Mazewski C, Schniederjan MJ, et al (2001). Neurofibromatosis-2 and spinal cord ependymomas: Report of two cases and review of the literature. Child's nervous system : ChNS : Official J of the International Society for Pediatric Neurosurgery;27:757-64.

Andre JB, Bammer R. (2010). Advanced diffusion-weighted magnetic resonance imaging techniques of the human spinal cord. Topics in magnetic resonance imaging : TMRI ;21:367-78.

Arguello F, Baggs, RB, Duerst RE et al (1990). Pathogenesis of vertebral metastasis and epidural spinal cord compression. Cancer 65, 98-106.

Arnautovi, K. and Arnautovic A (2009), Extramedullary intradural spinal tumors: a review of modern diagnostic and treatment options and a report of a series. Bosn J Basic Med Sci 9 Suppl 1: 40-5.

Arnautovic A and Arnautovic K (2014). Extramedullary Intradural Spinal Tumors." Contemporary Neurosurgery 36.5: 1-8.

Beall DP, Googe DJ, Emery R, et al. 2007). Extramedullary intradural spinal tumors: a pictorial review. Curr Probl Diagn Radiol 36(5):185-98

Bloomer CW. Ackerman A. Bhatia AG (2006), Imaging for spine tumors and new applications. Top Magn Reson Imaging 17(2): 69-87.

Bostrom A, Hans FJ, Reinacher PC, et al (2008). Intramedullary hemangioblastomas: timing of surgery, microsurgical technique and follow-up in 23 patients. European spine journal : official publication of the European Spine Society, the European Spinal Deformity Society, and the European Section of the Cervical Spine Research Society 17:882-6.

Bruna J, Gonzalez L, Miro Jet al (2009). Leptomeningeal carcinomatosis: prognostic implications of clinical and cerebrospinal fluid features. Cancer, 115(2): 381-9.

Bruna, J, Simo M, and Velasco R (2012). Leptomeningeal metastases. Curr Treat Options Neurol 14(4):402-15.

Buhmann Kirchhoff S, Becker C, Duerr HR et al (2009). Detection of osseous metastases of the spine: comparison of high resolution multi-detector-CT with MRI. Eur J Radiol 69: 567-73.

Cemil B, Gokce EC, Kirar F, et al (2012). Intramedullary spinal cord involvement from metastatic gastric carcinoma: a case report. Turkish neurosurgery 22:496-8.

Chai BB and Cho CH (2013) Cervical spine mass imaging: MRI or CT. Spine J 13:713-4.

Chamberlain MC, Eaton KD, Fink JR et al (2010). Intradural intramedullary spinal cord metastasis due to mesothelioma. Journal of neuro-oncology 97:133-6.

Chamberlain MC, Glantz M, Groves MD et al (2009). Diagnostic tools for neoplastic meningitis: detecting disease, identifying patient risk, and determining benefit of treatment. Semin Oncol 36(4 Suppl 2): S35-45.

Chamberlain, MC (2010). Leptomeningeal metastasis. Curr Opin Oncol, 22(6):627-35.

Chamberlain, MC (2008). Neoplastic meningitis. Oncologist, 13(9): 967-77.

Chen YJ, Chang GC, Chen WH et al (2007). Local metastases along the tract of needle: a rare complication of vertebroplasty in treating spinal metastases. Spine (Phila Pa 1976), 32, E615-8.

Cheung YK, Fung CF, Chan FL et al (1991). MRI features of spinal ganglioglioma. Clinical imaging 15:109-12.

Choi IJ, Chang JC, Kim DW et al (2012). A case report of "spinal cord apoplexy" elicited by metastatic intramedullary thyroid carcinoma. Journal of Korean Neurosurgical Society 51:230-2.

Chu BC, Terae S, Hida et al (2001). MR findings in spinal hemangioblastoma: correlation with symptoms and with angiographic and surgical findings. AJNR American journal of neuroradiology 22:206-17.

Clarke JL, Perez HR, Jacks LM et al (2010). Leptomeningeal metastases in the MRI era. Neurology 74(18):1449-54.

Colangeli S, Rossi G Ghermandi R et al (2010). Fluid-fluid levels detected on MRI and mimicking primary aneurismal bone cysts in a case of spinal bone metastasis. Eur Rev Med Pharmacol Sci 18:41-3.

Cook GJ, and Fogelman I (2000). The role of positron emission tomography in the management of bone metastases. Cancer 88:2927-33.

de Azevedo CR, Cruz MR, Chinen LT et al (2011). Meningeal carcinomatosis in breast cancer: prognostic factors and outcome. J Neurooncol 104(2): p. 565-72.

De Verdelhan O, Haegelen C, Carsin-Nicol B et al (2005). MR imaging features of spinal schwannomas and meningiomas. J Neuroradiol, 32(1): 42-9.

Dieteman JL, Correia Bernardo R, Bogorin A et al (2005). Normal and abnormal meningeal enhancement: MRI features. J Radiol 86(11):1659-83.

Ding DC, Chu TY (2010). Brain and intramedullary spinal cord metastasis from squamous cell cervical carcinoma. Taiwanese journal of obstetrics & gynecology 49:525-7.

Ducreux D, Fillard P, Facon D, et al (2007). Diffusion tensor magnetic resonance imaging and fiber tracking in spinal cord lesions: current and future indications. Neuroimaging clinics of North America 17:137-47.

Duong LM, McCarthy BJ, McLendon RE, et al (2012). Descriptive epidemiology of malignant and nonmalignant primary spinal cord, spinal meninges, and cauda equina tumors, United States, 2004-2007. Cancer 118:4220-7.

Duprez TP, Jankovski A, Grandin C, et al (2008). Intraoperative 3T MR imaging for spinal cord tumor resection: feasibility, timing, and image quality using a "twin" MR-operating room suite. AJNR American journal of neuroradiology 29:1991-4.

Duvauferrier R, Valence M, Patrat-Delon S (2013). Current role of CT and whole body MRI in multiple myeloma. Diagnostic and Interventional Imaging 94, Issue 2, 169–183

Fayad L, Blakeley J, Plotkin S (2013). Whole Body MRI at 3T with Quantitative Diffusion Weighted Imaging and Contrast-Enhanced Sequences for the Characterization of Peripheral Lesions in Patients with Neurofibromatosis Type 2 and Schwannomatosis. J ISRN Radiology vol. 2013.

Fischer S, Lee W, Aulisi E, Singh H (2007). Gliosarcoma with intramedullary spinal metastases: a case report and review of the literature. Journal of clinical oncology : official journal of the American Society of Clinical Oncology 25:447-9.

Fritz JV (2014). Neuroimaging trends and future outlook. Review. Neurol Clin 32(1):1-29

Garces-Ambrossi GL, McGirt MJ, Mehta VA, et al (2013). Factors associated with progression-free survival and long-term neurological outcome after resection of intramedullary spinal cord tumors: analysis of 101 consecutive cases. Journal of neurosurgery Spine 11:591-9.

Gasser T, Sandalcioglu IE, El Hamalawi B et al (2005). Surgical treatment of intramedullary spinal cord metastases of systemic cancer: functional outcome and prognosis. Journal of neuro-oncology 73:163-8.

Gauthier H, Guilhaume MN, Bidard FC, et al (2010). Survival of breast cancer patients with meningeal carcinomatosis. Ann Oncol; 21(11):2183-7.

Gomori JM, Heching N, Siegal T (1998). Leptomeningeal metastases: evaluation by gadolinium enhanced spinal magnetic resonance imaging. J Neurooncol 36(1): 55-60.

Gorgula A, Albayrak BS, and Kose T (2005). Cervical leptomeningeal and intramedullary metastasis of a cerebral PNET in an adult. J Neurooncol 74(3):339-40.

Gottfried ON, Gluf W, Quinones-Hinojosa A (2003). Spinal meningiomas: surgical management and outcome. Neurosurg Focus 14(6): e2.

Griffith JF, Guglielmi G (2010). Vertebral fracture. Radiol Clin North Am. 48(3):519-29.

Harrop JS, Ganju A, Groff M et al (2009). Primary intramedullary tumors of the spinal cord. Spine 34:S69-77.

Hashii H, Mizumoto M, Kanemoto A, et al (2011). Radiotherapy for patients with symptomatic intramedullary spinal cord metastasis. Journal of radiation research 52:641-5.

Henson JW (2001). Spinal cord gliomas. Current opinion in neurology 14:679-82.

Horger M, Ritz R, Beschorner R, et al (2011). Spinal pilocytic astrocytoma: MR imaging findings at first presentation and following surgery. European journal of radiology 79:389-99.

Houten JK, Cooper PR (2000). Spinal cord astrocytomas: presentation, management and outcome. Journal of neuro-oncology 47:219-24.

Imagama S, Ito Z, Wakao N, et al (2011). Differentiation of localization of spinal hemangioblastomas based on imaging and pathological findings. European spine journal : official publication of the European Spine Society, the European Spinal Deformity Society, and the European Section of the Cervical Spine Research Society 20:1377-84.

Ishii T, Terao T, Komine K, Abe T (2010). Intramedullary spinal cord metastases of malignant melanoma: an autopsy case report and review of the literature. Clinical neuropathology 29:334-40.

Jarraya M, Hayashi D, Lebreton C et al (2013). Isolated vertebral metastasis with a fl uid- fl uid level from a poorly differentiated adenocarcinoma. Diagn Interv Radiol 19: 233-6.

Jeon MJ, Kim TY, Han JM, et al (2011). Intramedullary spinal cord metastasis from papillary thyroid carcinoma. Thyroid : official journal of the American Thyroid Association 21:1269-71.

Kalayci M, Cagavi F, Gul S, et al (2004). Intramedullary spinal cord metastases: diagnosis and treatment - an illustrated review. Acta neurochirurgica 146:1347-54; discussion 54.

Kaplan JG, DeSouza T, Farkash A et al (1990). Leptomeningeal metastases: comparison of clinical features and laboratory data of solid tumors, lymphomas and leukemias. J Neurooncol 9(3): 225-9.

Kaya RA, Dalkilic T, Ozer F, Aydin Y (2003). Intramedullary spinal cord metastasis: a rare and devastating complication of cancer--two case reports. Neurolog medico-chirurgica 43:612-5.

Kesari S. and Batchelor TT (2003). Leptomeningeal metastases. Neurol Clin 21(1): 25-66.

Khoo MM, Tyler PA, Saifuddin A, et al (2001). Diffusion-weighted imaging (DWI) in musculoskeletal MRI: A critical review. Skeletal Radiol. 40(6):665-81.

Kim W, Min CK, Shim YS et al (2008). Intramedullary spinal cord metastasis of acute lymphoblastic leukemia as the initial manifestation of relapse. Leukemia & lymphoma 49:1214-6.

King AT, Sharr MM, Gullan RW et al (1998). Spinal meningiomas: a 20-year review. Br J Neurosurg 12(6): p. 521-6.

Klekamp Jand Samii M (1999). Surgical results for spinal meningiomas. Surg Neurol 52(6): 552-62.

Ko JK, Cha SH, Lee JH et al (2012). Intramedullary spinal cord metastasis of choriocarcinoma. J Korean Neurosurgical Society 51:141-3.

Koeller KK, Rosenblum RS, Morrison AL (2000). Neoplasms of the spinal cord and filum terminale: radiologic-pathologic correlation. Radiographics : a review publication of the Radiological Society of North America, Inc 20:1721-49.

Koeller KK, Rushing EJ(2004) From the archives of the AFIP: pilocytic astrocytoma: radiologic-pathologic correlation. Radiographics : a review publication of the Radiological Society of North America, Inc 24:1693-708.

Lane B (2003) Practical imaging of the spine and spinal cord. Topics in magnetic resonance imaging : TMRI 14:438-43.

Le Rhun E, Taillibert S, Chamberlain MC (2013). Carcinomatous meningitis: Leptomeningeal metastases in solid tumors. Surg Neurol Int, 4(Suppl 4): S265-88.

Lieberson RE, Veeravagu A, Eckermann JM, et al (2012). Intramedullary spinal cord metastasis from prostate carcinoma: a case report. Journal of medical case reports 6:139.

Liu X, Germin BI, Ekholm S (2011). A case of cervical spinal cord glioblastoma diagnosed with MR diffusion tensor and perfusion imaging. Journal of neuroimaging : Official J of the American Society of Neuroimag :292-6.

Liu, WC, Choi G, Lee SH et al (2009). Radiological findings of spinal schwannomas and meningiomas: focus on discrimination of two disease entities. Eur Radiol 19(11): 2707-15.

Long SS, Yablon CM, Eisenberg RL (2010). Bone marrow signal alteration in the spine and sacrum. AJR Am J Roentgenol 195:W178-200.

Lonser RR, Weil RJ, Wanebo JE, et al (2003). Surgical management of spinal cord hemangioblastomas in patients with von Hippel-Lindau disease. J of Neurosurg 98:106-16.

Louis DN, Ohgaki H, Wiestler OD, et al (2007). The 2007 WHO classification of tumours of the central nervous system. Acta neuropathologica 114:97-109.

Maccauro G, Spinelli MS, Mauro S et al (2011). Physiopathology of spine metastasis. Int J Surg Oncol, 107969.

MacCollin M, Chiocca EA, Evans DG et al (2005). Diagnostic criteria for schwannomatosis. Neurology 64(11): 1838-45.

Marliani AF, Clementi V, Albini-Riccioli L, et al (2007). Quantitative proton magnetic resonance spectroscopy of the human cervical spinal cord at 3 Tesla. Magnetic resonance in medicine : official journal of the Society of Magnetic Resonance in Medicine / Society of Magnetic Resonance in Medicine 57:160-3.

Mechtler LL and Nandigam K (2013). Spinal cord tumors: new views and future directions. Neurol Clin 31(1):241-68.

Mechtler L. (2009)Neuroimaging in neuro-oncology. Neur clin 27:171-201, ix.

Metser U, Lerman H, Blank A (2004). Malignant involvement of the spine: assessment by 18F-FDG PET/CT. J Nucl Med 45:279-84.

Miranpuri AS, Rajpal S, Salamat MS et al (2011). Upper cervical intramedullary spinal metastasis of ovarian carcinoma: a case report and review of the literature. Journal of medical case reports 5:311.

Morris PG, Reiner AS, Szenberg OR et al (2012). Leptomeningeal metastasis from non-small cell lung cancer: survival and the impact of whole brain radiotherapy. J Thorac Oncol. 7(2):382-5.

Padhani R, Koh DM, and Collins DJ (2011). Whole-body diffusion-weighted MR imaging in cancer: current status and research directions. Radiology 261(3):700–718.

Park JH, Kim YJ, Lee JO et al (2012). Clinical outcomes of leptomeningeal metastasis in patients with non-small cell lung cancer in the modern chemotherapy era. Lung Cancer, 76(3): 387-92.

Pattany PM, Saraf-Lavi E, Bowen BC (2003). MR angiography of the spine and spinal cord. Topics in magnetic resonance imaging : TMRI 14:444-60.

Plotkin SR, O'Donnell CC, Curry WT (2011). Spinal ependymomas in neurofibromatosis Type 2: a retrospective analysis of 55 patients. Journal of neurosurgery Spine 14:543-7.

Rodallec MH, Feydy A, Larousserie F (2008). Diagnostic imaging of solitary tumors of the spine: what to do and say. Radiographics 28:1019-41.

Ropper AE, Cahill KS, Hanna JW (2011). Primary vertebral tumors: a review of epidemiologic, histological, and imaging findings, Part I: benign tumors. Neurosurg 69: 1171-80.

Rudnicka H, Niwinska A, and Murawska M (2007). Breast cancer leptomeningeal metastasis--the role of multimodality treatment. J Neurooncol, 84(1):57-62

Rumpel H, Chong Y, Porter DA et al (2013). Benign versus metastatic vertebral compression fractures combined diffusion weighted MRI and MR spectroscopy aids differentiation. Eur Radiol 23(2):541-50

Runge VM, Lee C, Williams NM et al. (1997). Contrast-enhanced magnetic resonance imaging in a spinal epidural tumor model. Invest Radiol 32(10): 589-95.

Rossi A, Gandolfo C, Morana G et al (2007). Tumors of the Spine in Children Neuroimaging Clin of North America 17:1; 17-35

Ryan PJ and Fogelman I (1995). The bone scan: where are we now? Semin Nucl Med 25:76-91.

Rykken JB, Diehn FE, Hunt CH, et al (2013). Intramedullary spinal cord metastases: MRI and relevant clinical features from a 13-year institutional case series. 34(10):2043-9

Salvo N, Christakis M, Rubenstein J (2009). The role of plain radiographs in management of bone metastases. J Palliat Med 12:195-8.

Samii M, Klekamp J (1994). Surgical results of 100 intramedullary tumors in relation to accompanying syringomyelia. Neurosurgery 35:865-73; discussion 73.

Sandu N, Popperl G, Toubert ME, et al (2011). Current molecular imaging of spinal tumors in clinical practice. Molecular medicine 17:308-16.

Santi M, Mena H, Wong K et al (2003). Spinal cord malignant astrocytomas. Clinicopathologic features in 36 cases. Cancer 98:554-61.

Schijns OE1, Kurt E, Wessels P et al (2000). Intramedullary spinal cord metastasis as a first manifestation of a renal cell carcinoma: report of a case and review of the literature. Clin Neurol Neurosurg 102;4: 249–254.

Schwartz TH and McCormick PC (2000). Intramedullary ependymomas: clinical presentation, surgical treatment strategies and prognosis. Journal of neuro-oncology 47:211-8.

Seidenwurm DJ, Wippold FJ, 2nd, Cornelius RS, et al (2012). ACR Appropriateness Criteria((R)) myelopathy. Journal of the American College of Radiology : JACR 9:315-24.

Seo HS, Kin JH, Lee DH et al (2010). Nonenhancing intramedullary astrocytomas and other MR imaging features: a retrospective study and systematic review. AJNR Am J Neuroradiol. 31(3):498-503

Setzer M, Vatter H, Marquardt G et al (2007). Management of spinal meningiomas: surgical results and a review of the literature. Neurosurg Focus 23(4): E14.

Shah KC, Chacko G, John S et al (2005). Spinal intramedullary metastasis from intracranial germinoma. Neurology India 53:374-5.

Shah LM and Salzman KL (2011). Imaging of spinal metastatic disease. Int J Surg Oncol, 769753.

Simon T, Niemann CA, Hero B, et al (2012). Short- and long-term outcome of patients with symptoms of spinal cord compression by neuroblastoma. Dev Med Child Neurol 54(4):347-52.

Sivan M, Nandi D, Cudlip S(2006). Intramedullary spinal metastasis (ISCM) from pituitary carcinoma. Journal of neuro-oncology 80:19-20.

Smith AB, Soderlund KA, Rushing EJ (2012). Radiologic-pathologic correlation of pediatric and adolescent spinal neoplasms: Part 1, Intramedullary spinal neoplasms. AJR American J of roentgenology 198:34-43.

Smith JK, Lury K, Castillo M (2006). Imaging of spinal and spinal cord tumors. Seminars in roentgenology 41:274-93.

Soderlund KA, Smith AB, Rushing EJ et al (2012). Radiologic-pathologic correlation of pediatric and adolescent spinal neoplasms: Part 2, Intradural extramedullary spinal neoplasms. AJR Am J Roentgenol 198 (1): 44-51.

Stephen JH, Sievert AJ, Madsen PJ, et al. Spinal cord ependymomas and myxopapillary ependymomas in the first 2 decades of life: a clinicopathological and immunohistochemical characterization of 19 cases. Journal of neurosurgery Pediatrics 9:646-53.

Sugahara T, Korogi Y, Hirai T et al (1998). Contrast-enhanced T1-weighted three-dimensional gradient-echo MR imaging of the whole spine for intradural tumor dissemination. AJNR Am J Neuroradiol 19(9): p. 1773-9.

Sun L, Song Y, Gong Q (2013). Easily misdiagnosed delayed metastatic intraspinal extradural melanoma of the lumbar spine: A case report and review of the literature. Oncol Lett, 5, 1799-1802.

Sung WS, Sung MJ, Chan JH, et al (2012). Intramedullary Spinal Cord Metastases: A 20-Year Institutional Experience with a Comprehensive Literature Review. World neurosurgery

Tantongtip D and Rukkul P(2011). Symptomatic leptomeningeal and entirely intramedullary spinal cord metastasis from supratentorial glioblastoma: a case report. J Med Assoc Thai 94 Suppl 7:S194-7.

Theodorou DJ, Theodorou SJ, Sartoris DJ (2008). An imaging overview of primary tumors of the spine: Part 1. Benign tumors. Clin Imaging 32:196-203.

Tihan T, Chi JH, McCormick PC, et al (2006). Pathologic and epidemiologic findings of intramedullary spinal cord tumors. Neurosurgery clinics of North America 17:7-11.

Tinchon A, Oberndorfer S, Marosi C, et al (2012). Malignant spinal cord compression in cerebral glioblastoma multiforme: a multicenter case series and review of the literature. Journal of neuro-oncology 2:221-6.

Traul DE, Shaffrey ME, Schiff D (2007). Part I: spinal-cord neoplasms-intradural neoplasms. The lancet oncology 8:35-45.

van Aalst J,, Hoekstra F, Beuls EA, et al (2005). Intraspinal dermoid and epidermoid tumors: report of 18 cases and reappraisal of the literature. Pediatr Neurosurg 45(4): 281-90.

Vassiliou V, Papamichael D, Polyviou P, et al (2012). Intramedullary spinal cord metastasis in a patient with colon cancer: a case report. Journal of gastrointestinal cancer 43:370-2.

Vertinsky AT, Krasnokutsky MV, Augustin M, et al (2007). Cutting-edge imaging of the spine. Neuroimaging clinics of North America 17:117-36.

VIDAL JA and Murphey MD (2007). Primary tumors of the osseous spine. Magn Reson Imaging Clin N Am 15:239-55, vii.

Waldron JS and Cha S (2006). Radiographic features of intramedullary spinal cord tumors. Neurosurgery clinics of North America 17:13-9.

Wanebo JE, Lonser RR, Glenn GM, et al (2003). The natural history of hemangioblastomas of the central nervous system in patients with von Hippel-Lindau disease. Journal of neurosurgery 98:82-94.

Wand LX, LV FZ, MA et al (2012). Multifocal osteolytic lesions within lumbar spine in a middle-aged Chinese woman: a benign metastasizing leiomyoma? Spine (Phila Pa 1976) 37:E259-63.

Wang M, Dai Y, Han Y, et al (2011). Susceptibility weighted imaging in detecting hemorrhage in acute cervical spinal cord injury. Magn Reson Imaging 29: 365–73.

Wilson DA, Fusco DJ, Uschold TD, et al (2012). Survival and functional outcome after surgical resection of intramedullary spinal cord metastases. World neurosurgery 77:370-4.

Wilson PE, Oleszek JL, Clayton GH (2007). Pediatric spinal cord tumors and masses. J of spinal cord medicine 30 Suppl 1:S15-20.

Yuh WT, Quets JP, Lee HJ (1996). Anatomic distribution of metastases in the vertebral body and modes of hematogenous spread. Spine (Phila Pa 1976) 21: 2243-50.

ASN Scottsdale, AZ 2015

SPINE TUMORS

Laszlo L. Mechtler, MD, FAAN
Medical Director, DENT Neuro-Oncology Center
Chief of Neuro-Oncology
Roswell Park Cancer Institute
Neuroimager

EXTRADURAL TUMORS

Epidural Metastasis

Epidemiology

Epidural spinal cord compression (ESCC) by metastases is more common that compression by primary spinal tumors. It occurs in 5% of patients who die of cancer, which represents more than 25,000 cases annually of spinal cord compression in the United States. Moreover, prolonged survival time from improved cancer treatment is expected to increase the incidence of ESCC. Approximately one-half of ESCCs in adults are metastases from breast, lung, or prostate cancer; the primary tumor is not identified in 10% of cases (Table 58d.1).

Table 58D1: Types of primary tumors causing metastatic epidural spinal cord compression in men and women

	Men (%)	Women (%)
Lung	53	12
Breast	0	59
Prostate	8	---
Kidney	3	3
Melanoma	0	1
Gastrointestinal	5	3
Female reproductive	---	6
Miscellaneous	31	16

Source: Modified with permission from RJ Stark, RA Henson, SJW Evans. Spinal metastases—a retrospective survey from a general hospital. Brain 1982;105:189-213.

Distribution

The overall frequency of metastases to any portion of the spine is a function of length: 70% involve the thoracic spine, 20% the lumbosacral spine, and 10% the cervical spine. Lung and breast carcinomas tend to metastasize to the thoracic spine and color or pelvic tumors to the lumbosacral spine. Approximately 10-38% of epidural metastases involve multiple noncontiguous levels—an important consideration in evaluation and treatment.

The anatomical site of metastasis is an important factor in patient management. Bony lesions occur in more than 90% of patients with spinal metastasis, of which 71% are osteolytic, 8% are osteoblastic, and 21% are mixed. Eighty-five percent of metastases arise in the vertebral body and invade the epidural space anteriorly. Laminectomy can be effective in decompressing the spinal cord but fails to remove the tumor, which arises

from the anterior body of the vertebrae. Metastatic lesions never involve the intravertebral disc or transgress the dura.

Pathogenesis

Metastases cause ESCC by three mechanisms. The first and most common is hematogenous spread to the vertebra, which contains highly vascularized hematopoietic bone marrow and rich growth factors. Second is spread of tumor cells to the vertebral column through the vertebral venous (Batson's) plexus. Batson's veins are valveless and have low intraluminal pressure and allows retrograde tumor seeding when intrathoracic or intra-abdominal pressure increases (i.e., through coughing, sneezing, or Valsalva's maneuver). The third mechanism of direct invasion of tumor through the intravertebral foramina is responsible for approximately 15% of ESCCs. Lymphoma accounts for about 75% of these cases, in which radioisotope studies and radiographs are typically normal.

Clinical Features

Pain, the most common initial feature, occurs in 95% of adults and 80% of children. Pain is usually localized to the site of metastasis and is caused by stretching the pain-sensitive bony periosteum. Radicular pain is less frequent but is also localizing. It is often bilateral in thoracic ESCC and unilateral in cervical and lumbosacral ESCC. Segmental or funicular pain, indicating intrinsic spinal cord damage, is uncommon and is continuous, burning, dull, and diffuse. As degenerative disc disease, Valsalva's maneuver, straight-leg raising, and neck flexion aggravate back pain. Unlike a herniated disc, ESCC pain is characteristically aggravated by recumbency (which is worse at night). Epidural metastasis is the initial manifestation of malignancy in about 10% of patients. The primary is usually lung cancer, myeloma, lymphoma, or renal cell cancer.

Common clinical features at the time of diagnosis are bilateral weakness (76%), autonomic dysfunction (57%), and sensory complains (51%). Weakness (caused b anterior compressions of the spinal cord) precedes the sensory symptoms. At the time of diagnosis, 50% of patients are ambulatory, 35% are paraparetic, and 15% are paraplegic. As many as one-half of those who are paraplegic at diagnosis, had deteriorated abruptly or within the previous 24- to 48-hour period. Rapid progression is mostly seen in patients with lung cancer, lymphoma, or renal tumors. Autonomic dysfunction is never the presenting symptom. Sensory complains are almost always painful. Lhermitte's sigh, herpes zoster, gain ataxia, and Brown-Sequard's syndrome are unusual in ESCC.

Neuroimaging

On plain radiographs of the spine, metastases cause changes in the pedicles, which are compact bone, before the vertebral bodies, which must be 50% destroyed before changes can be identified. Abnormal radiographs at the time of presentation are seen in 85% of patients with ESCCs from epithelial tumors but in only 33% of patients with lymphoma. The most common findings are pedicle erosion ("winking owl" sign), paravertebral soft issue shadow, vertebral collapse, and pathological fracture dislocation. The likelihood of epidural tumor is 87% when vertebral compression is greater than 50%. ESCC is present in only 7% of patients with radiological evidence of vertebral metastases without collapse.

The sensitivity of bone scanning approaches 91%, but its specificity is limited, with a high false-positive rate. Computed tomography (CT) of the spine is more sensitive and specific than plain radiographs or radionuclide scanning for ESCC. The combination of myelography followed by CT was the study of choice but is being replaced by magnetic resonance imaging (MRI). MRI is as sensitive as bone scans for detecting vertebral metastasis and is more specific.

MRI provides detailed anatomical resolution of the vertebrae and surrounding structures and permits direct visualization in multiplanar sections along the entire length of the spinal column. Unenhanced T1- weighted sagittal images are obtained first because contract enhancement might obscure subtle vertebral metastases. This is followed by a T2-weighted or enhanced T1-weighted scan. The characteristic findings on MRI are multiple foci of low signal intensity on T1-weighted images. Collapse and destruction of the vertebral body sparing the

adjacent disc spaces are common. Short T1 inversion recovery, which is a fat-suppression technique, increases the sensitivity of MRI. Although gadolinium enhancement may mask vertebral lesions, it is helpful in the detection and characterization of epidural, intradural, and intramedullary processes. Conventional myelography is preferred to MRI in patients who cannot lie still because of claustrophobia or severe pain and in patients with severe scoliosis, ferromagnetic implants, aneurysm clips, or a cardiac pacemaker. In cases in which MRI does not yield the diagnosis, myelography should be performed.

Prognostic Variables

Severity of weakness at time of diagnosis is the most significant prognostic variable for recovery of neurological function. Ninety percent of patients who are ambulatory at diagnosis remain ambulatory after treatment. After radiation, 75% of paraparetic patients with radiosensitive tumors remain ambulatory, whereas only 34% with radioresistant tumors remain ambulatory. In contrast, only 13% of paraplegic patients with radiosensitive tumors and none with radioresistant tumors become ambulatory. Rate of onset and progression of symptoms correlate better with outcome than does duration. Outcome also depends on the radiosensitivity of the primary tumor. Myeloma, lymphoma, neuroblastoma, and to a lesser degree, breast and prostate cancer, have a more favorable prognosis; non-small cell lung cancer, renal cancer, and melanoma have a poor prognosis. The extent and location of epidural disease also influence the response to treatment. Vertebral collapse and anterior location of the metastasis is less favorable because surgical access is limited, and a partial myelographic block has a more favorable prognosis for neurological recovery than a complete block.

Treatment

ESCC is usually associated with inadequate control of the primary tumor, and survival time is short. Treatment of ESCC is palliative and directed at maintaining ambulation, decreasing tumor bulk, and relieving pain. Patients with advanced cancer and poor performance status are treated conservatively. In those without advanced disease, expeditious diagnosis and treatment should improve or at least maintain neurological function. High-dose corticosteroids are started immediately, followed by radiotherapy and sometimes chemotherapy. Corticosteroids rapidly decrease spinal cord vasogenic edema and promote clinical improvement in relation to dose administered. Dexamethasone, 100 mg intravenously followed by 24 mg every 6 hours, is recommended. The usual maintenance dose is 4 mg every 6 hours. An intravenous bolus of high-dose dexamethasone may cause severe but transitory (5-minute) dysesthesias of the genitalia. Other side effects include hiccoughs, psychosis, hallucinations, hyperglycemia, gastrointestinal bleeding, and drug interaction (phenytoin and Warfarin).

Recommendations conflict for the treatment of ESCC. Historically, decompressive laminectomy had been the most common treatment for ESCC. Improved outcomes have also been obtained with the combination of laminectomy and radiotherapy. Other studies showed no difference between radiotherapy and laminectomy plus radiotherapy. Radiotherapy alone is now the treatment of choice. Patients with radiosensitive tumors (e.g., lymphoma, seminoma, myeloma, Ewing's sarcoma, and neuroblastoma) respond, but patients with radioresistant tumors (e.g., lung, colon, renal, and melanoma) also respond as well to radiotherapy alone as to combined surgery and radiation. The recommended radiation fields are two normal vertebral bodies above and below the margins of epidural tumor. Because epidural metastasis may occur at multiple levels, the entire spinal cord must be visualized by MRI or myelography. The frequency of local recurrence after initial response, independent of histology, is approximately 10%. Most radiation oncologists recommend 3,000 cGy over 10 fractions. If the irradiated volume is large or if the tumor is highly radiosensitive, a smaller daily dose is usually used.

Decompressive laminectomy is indicated in patients with a posteriorly situated epidural metastasis in the absence of vertebral disease. ESCC in children is often from tumors (e.g., neuroblastoma) that invade the spinal canal through the neural foramen. In this situation, decompressive laminectomy may be effective. Because metastatic tumor is anterior to the cord in 85% of cases, vertebral body resection followed by stabilization offers the best results. The reported surgical morbidity is 9%, but the ambulation rate increased from 28% to 80% postoperatively, and median survival is 16 months. Postoperation radiation therapy is required (Table 58D.2).

Table 58D.2: Indications for surgical intervention in epidural spinal cord compression

Need for tissue diagnosis
Spinal instability
Progressive deterioration during chemotherapy or radiotherapy
Recurrent disease in previously irradiated site
Rapidly progressive cord compression by a known radioresistant tumor

Source: Modified with permission from N Sundaresan, HH Schmidek, AL Schiller, et. al. Tumors of the Spine: Diagnosis and Clinical Management. Philadelphia: Saunders, 1990.

With few exceptions, ESCCs do not respond to chemotherapy rapidly enough to prevent neurological deterioration. Systemic chemotherapy can be used to treat chemosensitive tumors with stable or slowly progressive neurological deficits because such epidural tumors are not protected by the blood-brain barrier. The best results have occurred with small cell tumors, such as lymphoma, germ cell tumors, neuroblastoma, or Ewing's sarcoma. Chemotherapy or hormonal therapy also may be effective in breast and prostate cancer. Some promising results have been achieved with systemic chemotherapy in children with chemosensitive tumors, but further studies are needed.

Overall, tumor type is a more important determinant of the functional outcome that type of treatment. The life expectancy of patients with bronchogenic carcinoma is 87 day; for breast cancer, it is 7 months; and for hematological malignancies, it is 12 months.

Extradural Primary Spinal Neoplasms

Tumors of the vertebral column, unlike tumors of all other bones, are more often malignant that benign. Myeloma is the only common primary tumor of the spine in adults. Neuroblastoma and Ewing's sarcoma are the main malignant spinal tumors of childhood, and despite substantial morbidity with early treatment, the outcome is often favorable because these tumors are relatively sensitive to radiations and chemotherapy.

Multiple myeloma is a plasma cell neoplasm that accounts for up to 33% of bone tumors. The peak incidence is in the sixth through eighth decades. It is twice as common in African-Americans as in Americans of European ancestry. Polyneuropathy is sometimes associated and confused the diagnoses of spinal cord compression. ESCC occurs in 10-15% of people with multiple myeloma. The median age of onset of plasmacytomas is 50 years, and the male-to-female ratio is 3 to 1. Most plasmacytomas evolve into multiple myeloma after 10 years. Radiation and chemotherapy remain the treatments of choice.

Ewing's sarcoma accounts for nearly 20% of spinal cord compression in children. Osteosarcoma and neuroblastoma are next in frequency. Neuroblastoma is the most common cause of spinal cord compression in children less than 5 years of age. Intensive chemotherapy and radiotherapy are beneficial in the treatment of Ewing's sarcoma, neuroblastoma, and osteosarcoma. Chordomas arise from notochordal remnants. Their location is the sacrococcygeal area in 50% of cases and the skull base in 35%. Chordomas are the second most common tumors of the spine. Peak incidence is the fifth through seventh decades (the same as that for metastatic cancer). Hematogenous dissemination occurs in 33% of cases. Surgery, the primary therapy, is followed by radiation when resection is incomplete.

INTRADURAL TUMORS

Leptomeningeal Metastasis

Leptomeningeal metastasis (LM) occurs when tumor cells infiltrate the arachnoid and the pia mater (leptomeninges), causing focal or multifocal infiltration. LM develops in approximately 5-8% of patients with non-Hodgkin's lymphoma and up to 70% of patients with leukemia. Adenocarcinomas are the most common

solid tumors causing LM. Breast cancer is first, followed by lung, melanoma, and gastrointestinal cancers. The prevalence of LM is increased in long-term survivors of melanoma and small cell lung cancer.

Untreated primary central nervous system (CNS) tumors, such as medulloblastoma, ependymoma, and glioma, also have high frequency of LM. CNS prophylaxis has markedly decreased the risk of Lm in leukemia. The risk factors for leptomeningeal lymphomatosis in non-Hodgkin's lymphoma are bone marrow and testicular involvement, extranodal disease, epidural invasion, diffuse histology, Burkitt's syndrome, and lymphoblastic histology. Most primary CNS lymphomas are parenchymal, often leading to leptomeningeal spread, whereas systemic lymphomas are primary meningeal with secondary parenchymal invasion.

Pathology

The characteristic pathologic features of LM are thin, sheetlike layers of tumor cells, multifocal nodules, infiltration of cranial or spinal nerve roots (or both), and superficial invasion of the brain and spinal cord through the Virchow-Robin spaces. Tumor infiltration is more prominent along the ventral surface of the brain and the dorsal surface of the spinal cord. LM is associated with a high frequency of brain metastasis (42%) and dural metastasis (16-37%). ESCC is seen in 1-5% of patients with LM. Most breast or lung cancers that cause LM have spread directly from vertebral or paravertebral metastasis, whereas gastrointestinal cancer invades through the perineural spaces. Deep CNS parenchymal metastasis occurs through hematogenous spread.

Clinical Features

The clinical features of LM are referable to the cerebrum, cranial nerves, or spinal nerve roots, individually and in combination. The features of cranial nerve involvement, in order of decreasing frequency, are ocular motor palsies, facial weakness, hearing loss, vision loss, facial numbness, and tongue deviation. Headache and encephalopathy are common. Seizures occur in 6% of patients. In the spine, the lumbosacral roots are most commonly involved. This results in a cauda equina syndrome of asymmetrical weakness, dermatomal sensory loss, and paresthesias. Pain is an initial symptom in 25% of patients.

The pathophysiology of clinical symptoms and signs of LM may be due to hydrocephalus, parenchymal invasion, ischemia, metabolic competitions, immune responses, and disruption of the blood-brain barrier.

Examination of the cerebrospinal fluid (CSF) is the most important test for LM. Only 3% of initial lumbar punctures yield normal CSF. The abnormalities, in order of decreasing frequency, are increased protein concentration, lymphocytic pleocytosis, increased CSF pressure, and positive cytology. The glucose concentration is decreased in 31% of patients. Cytological examination is the most specific test. Positive cytology is seen on initial CSF examination in 54% of cases, and the yield increases to above 90% when three separate spinal taps are performed (Table 58D.3). The best yield is obtained when CSF is taken from the symptomatic area. False-negative CSF cytology results are common, but they can be minimized by good technique. This involves withdrawing at least 10.2 ml of CSF for cytological analysis, processing the CSF specimen immediately, obtaining CSF from the site of known leptomeningeal disease, and repeating the procedure at least once after initial cytology is negative (Glantz et al. 1998). CSF markers, such as carcinoembryonic antigen, B-glucuronidase, B2-microglobulin, and lactate dehydrogenase are more useful for following the response to treatment that for initial diagnosis.

Newer techniques for diagnosing LM include flow cytometry and monoclonal antibodies. Polymerase chain reaction techniques have increased the sensitivity in diagnosis of lymphomatous meningitis. This technique is based on detection of clonal rearrangements of immunoglobulin or T-cell receptor genes (Rhodes et al. 1996).

Table 58D.3: Leptomeningeal metastases from solid tumors in 90 patients: cerebrospinal fluid (CSF) findings

	Initial (%)	Subsequent (%)
Pressure >160 mm CSF	50	71
Cells >5/ul	57	70
Protein >50 mg/dl	81	89
Glucose <40 mg/dl	31	41

Positive cytology	54	91
Normal	3	1

Source: Reprinted with permission from WR Wasserstrom, JP Glass, JB Posner. Diagnosis and treatment of leptomeningeal metastases from solid tumors: experience with 90 patients. Cancer 1982;49:549-772.

Neuroimaging

Gadolinium-enhanced MRI is the modality of choice and has almost twice the sensitivity of CT myelography. MRI shows thin, linear enhancement on the surface of nerve roots and the spinal cord. Sensitivity may be increased with high-dose contrast studies. Enhanced spinal MRI may detect LM in about one-half of patients who are at high risk of CSF seeding with a negative initial CSF cytology or no spinal symptoms. Treatment should be initiated on the basis of MRI even when CSF cytology is normal, if the clinical setting is supportive of LM (Gomori et al. 1998).

Treatment

The median survival of untreated patients with LM is 4-6 weeks. Most patients die from progressive neurological dysfunction. Radiotherapy is combined with intrathecal and systemic chemotherapy. Radiation therapy is delivered to the symptomatic site at a dose of 2,000-3,000 cGy in 10-15 fractions. Total cranial-spinal axis radiotherapy is used only for mengeal leukemia because of myelosuppression. Intrathecal therapy is favored because systemic chemotherapy is probably not as effective in treating LM from solid tumors. An intraventricular reservoir is the recommended method to deliver intrathecal chemotherapy because it provides a more uniform distribution of drug in the CSF. It is also allows frequent repetitions of low dosages of chemotherapeutic agents by means of a "concentration x time" regimen, which theoretically improves effectiveness without increasing toxicity. This is especially important when using methotrexate and cytosine arabinoside because they are cell cycle-specific agents and need fairly constant CSF levels to be effective. Methotrexate, 12-20 mg reconstituted in preservative-free sterile normal saline, is the mainstay of intrathecal chemotherapy for solid tumors. Cytosine arabinoside (ara-C), 30-100 mg, is substituted or added to methotrexate in LM from lymphoma or leukemia. Among patients with leukemia and lymphoma, 75-80% show a CSF response or clinical response to intrathecal chemotherapy, but patients with solid tumors, such as breast cancer, have a 40-80% response rate and a median survival of 6-7 months. The overall response rate for non-small cell lung cancer and melanoma is less than 20%.

With radioisotope ventriculography, more than 60% of patients show ventricular outlet, spinal, or convexity blocks due to leptomeningeal seeding. CSF flow blocks, when untreated, increase morbidity by increasing neurotoxicity (high-concentration effect), and increase CSF tumor progression (protective site effect), and increase systemic toxicity (reservoir effect). These flow abnormalities may be corrected with appropriately directed radiotherapy. Intrathecal chemotherapy should be delayed if abnormal flow is documented until appropriate radiotherapy re-establishes normal flow (Chamberlain and Kormanik 1996).

Intradural Extramedullary Primary Neoplasms

Most primary intradural extramedullary neoplasms are histologically benign tumors, such as meningiomas (25%), nerve sheath tumors (29%), and developmental tumors (epidermoids, dermoids, lipomas, and teratomas) (Table 58D.4).

Meningiomas

Most meningiomas arise from arachnoid cells. More than 90% are intradural, 6% are both intradural and extradural, and 7% are only extradural. Multiple meningiomas are rare except in patients with neurofibromatosis type 2. The peak incidence of meningiomas is between ages 40 and 70 years; 85% are in

women, and 80% are located in the thoracic spine. Meningiomas in men are commonly located in the cervical spine, tend to grow rapidly, and have an intradural and extradural component.

The initial symptom of spinal meningiomas, like other spinal tumors, is usually pain followed by paraparesis and sensory disturbances. The average duration of symptoms from onset to diagnosis is 23 months. Bone is not often affected, and only 10% have radiographic abnormalities. Myelography shows a characteristic displacement of the spinal cord away from the mass and enlargement of the subarachnoid space above and below the tumor. Meningiomas have a homogeneous appearance on MRI and are usually isointense to spinal cord on T1-weighted and T2-weighted sequences. Surgery is the treatment of choice. The recurrence rate is 13% after 10 years.

Table 58D.4: Mayo Clinic classification of 1,322 primary tumors of the spinal canal

Type	Frequency (%)
Neurilemomas (schwannomas)	29.0
Meningioma	25.5
Glioma (astrocytoma, ependymoma)	22.0
"Sarcoma" (lipomas, fibrosarcoma, chondromas, lymphomas)	11.9
Vascular tumors	6.2
Chordoma	4.0
Epidermoid, dermoid, teratomas	1.4

Source: Modified with permission from JL Sloof, JW Kernohan, CS MacCarty. Primary Intramedullary Tumors of the Spinal Cord and Filum Terminale. Philadelphia: Saunders, 1964.

Nerve Sheath Tumors

Nerve sheath tumors are schwannomas and neurofibromas. Schwannomas (neurilemomas) are composed of Schwann cells and produce an eccentric enlargement of the involved nerve root. Neurofibromas are a mixture of Schwann cells and fibroblasts with abundant collagen fibers and cause diffuse enlargement of the nerve root. Nerve sheath tumors comprise 29% of primary spinal cord tumors.

Nerve sheath tumors are evenly distributed along the spinal axis. Men and women are equally affected. Age at onset is usually between 31 and 60 years; average age is 43.5 year for nerve sheath tumors and 53 years for spinal meningiomas. Two-thirds of tumors are intradural, and of the remainder, one-half are dumbbell-shaped (intra-extradural) and one-half are extradural.

Pain is the initial feature in 75% of patients. It may be axial, radicular, or referred (distant nondermatomal pain). Pain is exacerbated by Valsalva's maneuver, coughing, sneezing, and recumbency. Mean duration of symptoms before diagnosis averages 1-4 years. Weakness and sensory symptoms predominate at the time of diagnosis; sphincter dysfunction is uncommon. Malignant deterioration of neurofibromas (neurofibrosarcoma) occurs in 3-13% of all cases; one-half of those are people with neurofibromatosis.

Radiographs of the spine are abnormal in 50% of cases. The usual finding is widening of the intervertebral foramen, erosion of the pedicle or vertebral body, and widening of the interpedicular distance. CT, myelography, or MRI provides a definitive image. Intradural schwannomas are usually hypointense on T1-weighted images and hyperintense on T2-weighted images. Ringlike enhancement is considered a sign of cystic degeneration and is more consistent with schwannoma that meningioma.

Embryonal Tumors

Embryonal tumors (epidermoid, dermoid cysts, teratomas, and lipomas) comprise 1-2% of primary spinal tumors. They are usually found in the lumbar region and associated with spina bifida occulta, posterior dermal sinuses, syringomyelia, or diastematomyelia. Associated cutaneous abnormalities may be found, including hypertrichosis, pigmented skin, sacral dimple, and cutaneous angiomas. Most lipomas are in the

cervicothoracic region and are intramedullary as well as intradural-extramedullary. MRI shows high signal-intensity T2-weighted images.

Intramedullary Spinal Cord Tumors

Intramedullary spinal cord tumors, both primary and metastatic, account for 2-4% of adult and 10% of pediatric CNS tumors. Glial tumors account for 22% of primary intraspinal tumors, the third most common after schwannomas and meningiomas. Astrocytomas and ependymomas account for 80-90% of all intramedullary tumors at all ages; in adults, ependymomas are more common than astrocytomas, whereas in children, ependymomas are more common than astrocytomas. Pediatric intramedullary astrocytic tumors are usually in the cervical cord, but some tumors extend the entire length of the cord (holocord astrocytomas). The McCormick Clinical and Functional Classification Scheme is used to prognosticate and quantify the results of treatment. (Table 58D.5).

Table 58D.5: McCormick clinical/functional classification scheme

Grade	Definition
I	Neurologically normal; mild focal deficit not significantly affecting function of involved limb; mild spasticity or reflex abnormality; normal gait.
II	Presence of sensorimotor deficit affecting function of involved limb; mild to moderate gait difficulty; severe pain or dysesthetic syndrome impairing patient's quality of life; still functions and ambulates independently.
III	More severe neurological deficit requires cane or brace for ambulation or significant bilateral upper extremity impairment; may or may not function independently.
IV	Severe deficit; requires wheelchair or cane or brace with bilateral upper extremity impairment; usually not independent.

Ependymoma

One-half of all ependymomas are located below the foramen magnum and involve either the spinal cord (55%) or the cauda region (45%), which includes the conus medullaris, filum terminale, and cauda equina. Myxopapillary ependymomas are characteristically seen in the region of the filum terminale and originate from islands of ependymal cells within fibrous band. The male-to-female ratio of spinal ependymomas is 2 to 1, and the median age of onset is 36 years. MRI has reduced the duration from symptom onset to diagnosis from 24-36 months to 14 months, and as a consequence, the frequency of weakness and sphincter involvement has decreased. The main complaint (95%) at the time of diagnosis is back pain. Most patients have dysesthesias without sensory loss. This is attributed to the location of the crossing spinothalamic tracts (central cord syndrome). When pain and numbness occur in a radicular pattern involving the legs, the underlying tumor is usually a myxopapillary ependymoma involving either the filum or the conus.

MRI, with and without contrast, is the imaging modality of choice for detecting intramedullary tumors. Ependymomas have a homogeneous enhancement pattern with sharply defined rostral and caudal poles; 30% have rostral-caudal cysts. Hypointensity at the tumor margins on both T1- and T2-weighted images indicates a relatively firm pseudocapsule, which should suggest ependymomas. Transverse T1-weighted gadolinium-enhanced MRI shows symmetric cord enlargement and intense, homogeneous enhancement.

Ependymomas, unlike astrocytomas, have a cleavage plane and tend not to invade normal tissue. Most ependymomas can be debulked with minimal morbidity. Patients with leg weakness usually show significant spinal cord thinning at surgery, which makes further excision hazardous. The common postoperative complications are a temporary increase in dysesthesias and a loss of proprioception. Postoperative radiotherapy is not indicated after total resection but should be done when MRI shows residual tumor or the histology indicates an anaplastic ependymoma. The 10-year survival rate is greater than 90%, with especially good results in patients with myxopapillary tumors.

Astrocytoma

Excluding cauda equina tumors, astrocytoma is the most common intramedullary spinal tumor in all ages; in children, astrocytoma is twice as common as ependymoma. The peak incidence is in the third to fifth decade of life. The average age at onset is 40 years for low-grade astrocytoma and 31 years for malignant astrocytoma. Overall, more than 75% are low-grade gliomas. Malignancy is more common in adults than in children. The distribution of astrocytomas is consistent with the length of cord segments; most are in the thoracic region. Up to 40% of astrocytomas have an associated intratumoral cyst or syringomyelia.

The clinical features of spinal cord astrocytoma are localized back pain initially, followed by progressive weakness. Unlike ependymomas, paresthesias are more common than dysesthesias. The duration of symptoms before diagnosis is 41 months for low-grade astrocytomas and 4-7 months for malignant astrocytomas. Unlike most intracranial low-grade astrocytomas, spinal astrocytomas enhance with gadolinium. MRI shows a patchy, heterogeneous pattern of enhancement consistent with a diffusely infiltrating tumor. Axial MRIs usually show asymmetric expansion of the cord. Astrocytomas are solitary, except in patients with NF-2. Malignant astrocytomas spread through the subarachnoid pathways and seed the leptomeninges. The complete spine and brain must be fully imaged to establish a treatment plan.

Therapy for intramedullary astrocytomas is controversial. Innovations in neurosurgery, such as bipolar coagulating forceps, operating microscopes, intraoperative ultrasonography, and the Cavitron ultrasonic surgical aspirator, have greatly increased the respectability of astrocytomas. However, the small number of cases and the indolent natural history of the tumor make evaluation of treatment efficacy difficult. Postoperative adjuvant therapy is not needed when gross total resection is achieved, but postoperative radiation is recommended after subtotal resection. Tumor recurs in children receiving 4,500 cGy of radiation, which suggests that this dose is not curative. The 5-year survival rate with low-grade astrocytoma is greater than 90%. The mean survival time for anaplastic astrocytoma and glioblastoma multiforme is less then 1 year, despite surgery, radiotherapy, and chemotherapy. Radical surgery is not indicated.

Intramedullary Metastasis

Intramedullary spinal cord metastasis accounts for 6% of myelopathies in cancer patients. The primary cancers responsible for intramedullary metastasis are lung (49%), breast (15%), lymphoma (9%), colorectal (7%), head and neck (6%), and renal (6%). There is a relative tendency for small cell lung carcinoma to metastasize to the spinal cord.

Intramedullary spinal metastases are thought to be arterially disseminated, a notion that is supported by the fact that one-half of patients have brain metastases. The conus medullaris is the most commonly affected segment, with 12.5% of patients having multilevel disease.

Three-fourths of patients develop significant neurological deficits within 1 month. The most common initial features are weakness, sensory deficits, urinary incontinence, and pain. Weakness from intramedullary metastasis is usually asymmetrical, whereas weakness from ESCC is relatively symmetrical. MRI is the investigation of choice. Focal beam radiation is recommended. The prognosis is poor, with 80% expected to die within 3 months.

REFERENCES

Chamberlain MC, Kormanik PA. Prognostic significance of Illindium-DTPA CSF flow studies in leptomeningeal metastases. Neurology 1996;46:1674-1677.

Glantz MJ, Cole BF, Glantz LK, et al. Cerebrospinal fluid cytology in patients with cancer: minimizing false negative results. Cancer 1998;82:733-739.

Gomori JM, Heching N, Siegal T. Leptomeningeal metastases: evaluation by gadolinium-enhancing spinal magnetic resonance enhanced imaging. J Neurooncol 1998;36:55-60.

Rhodes CH, Glantz MJ, Glantz LK, et al. A comparison of polymerase chain reaction examination of cerebrospinal fluid and conventional cytology in the diagnosis of lymphomatous meningitis. Cancer 1996;77:543-548.

Schiff D, O'Neill BP. Intramedullary spinal cord metastasis: clinical features and treatment outcome. Neurology 1996;47:906-912.

BENIGN BONE LESIONS OF THE SPINE

LESION	LOCATION	INCIDENCE	AGE	IMAGING	CLINICAL
Hemangioma	Vertebral body (T, L>C)	Most common benign spinal neoplasm	All Peak 4^{th}-6^{th} decade	CT:"polka dot" body MR:"white spot" on T1WI	Not painful Rarely can fracture
Osteoid Osteoma	Neural arch (L, C>T)	Common (10%) in spine	10 to 20 years	Dense sclerosis, lucent <2 cm	Painful, ASA sensitive
Osteoblastoma	Neural arch C>L, T; sacrum	Uncommon (40% in spine)	<30 years	Expansile lytic mass; +/-matrix mineralization	Scoliosis
Giant cell tumor	Vertebral body (sacrum >> vertebrae)	Uncommon	20s to 40s	Lytic, expansile, destructive, highly vascular	Malignant transformation
Osteochondroma	Spinous, Transverse Processes (10% to 12% multiple)	Common (rare in spine)	5 to 30 years	Pedunculated/sessile lesion; periosteum, cortex, marrow in continuity with host bone; cartilaginous CAP +/- Ca	Rarely symptomatic
Aneurysmal bone cyst	Posterior elements (C, T most common)	Rare (20% in spine)	80%< 20 year	Multiloculated, expansile; eggshell-like rims; blood products with fluid-level; highly vascular	Recurrence following resection is common. Can expand quickly
Eosinophilic granuloma		Uncommon	1^{st} or 2^{nd} decade	Vertebral body collapse (vertebra plana)	Fever; lung involvement
Epidural Lipomatosis	T-Spine	Rare		Fat in epidural space	Weakness; back pain; cortico-steroids

Cervical Spine

Syringomyelia and Hydromyelia
- Congenital syrinx often associated with Chiari malformation and other congenital anomalies (i.e. block vertebrate). Haustrations within cyst are typical of this type.
- Can also see a syrinx with trauma or as part of a cervical spine tumor. To exclude tumor, a syrinx should be enhanced with gadolinium

Transverse Myelitis
- T2 weighted bright sign in cord not associated with bone compression. Lesions will often enhance. Impossible to distinguish lesion of MS from monophasic transverse myelitis that can follow viremia

B-12 Deficiency
- Uncommon but dramatic cause of bright signal within the cord

Radiation Myelopathy
- Long segment of hyperintensity with T2 weighting

Rheumatoid Arthritis
- Pannus formation involves hypertrophy of ligamentous structures surrounding odontoid And along with atlanto-axial subluxation can cause narrowing at craniovertebral junction. Should be suspected in all cases of myelopathy in patients with rheumatoid arthritis.

Malignant Bone Lesions of Spine

Primary
- Myeloma
  - Most common primary malignant bone tumor
  - Pedicles involved late
  - Bone scan often negative
  - Multiple irregular lytic foci – No sclerotic rim
  - Generalized osteoporosis
- Lymphoma
  - Often associated with little bone destruction
  - Epidural mass often extends beyond one segment
  - Can simulate a lateral disc
- Chordoma
  - Arise from intraosseous notochordal remnants
  - Two types: typical and chondroid chordoma
  - Any age; incidence is 50-60 years
  - Preferential location for both ends of axial skeleton
    - 50% sacrum/coccyx
    - 35% skull base
    - 15% vertebral bodies
  - NECT scans show lytic, destructive lesions; Ca ++ in 30% to 70%; soft tissue mass often associated

Inhomogenous signal on MR; typical Chordomas are often very hyperintense on PD/T2WI
Males > females

Benign versus malignant compression fractures
Benign (osteoporotic) compression fracture
Signal similar to other vertebral bodies (in elderly, marrow is usually high signal on T1WI, low on T2WI
Signal is relatively uniform

Pathologic compression fracture
Lesions often multiple
Signal usually different from other vertebral bodies
Often Hypointense on T1WI, hyperintense on T2WI
Signal usually heterogenous
Pedicle involvement common

Metastatic source
Breast
Lung
Prostate
Lymphoma
Melanoma
Renal Cancer
Myeloma

Statistics
Most common extradural malignant spine tumor
Occur at death in 40% of patients dying of disseminated cancer

Location
Posterior vertebral body – Pedicle
Lower thoracic and lumbar area most common

Imaging Findings
Low Signal T1 (normal fat replaced)
Isointense to bright T2 – depends on amount of necrosis, hemorrhage, fibrosis

Caution: Magnevist can make bone tumors isointense

Intradural Extramedullary Tumors

A. Nerve sheath tumors
Most common intradural extramedullary mass
Types
Schwannoma, neurofibromas; ganglioneuroma, neurofibrosarcoma are rare
Primary seen in middle-aged adults
Variable location
Intradural extramedullary (70% to 75%)
"Dumbbell" (15%)
Extradural (15%)

Intramedullary (<1%)
Multiple lesions common with neurofibromatosis
Clinical symptoms can mimic disk herniation
Imaging findings
Enlarged neural foramen common, Ca ++ rare
75% isointense, 25% heperintense on T1WI
>95% hyperintense on T2Wi ("target" appearance common)
Virtually 100% enhance

B. Spinal meningioma
Most are typical benign meningioma
Second most common cause of spinal tumor
Classic patient is a middle-aged woman
Most common location: thoracic spine
90% are intradural extramedullary
Imaging findings
Bone erosion, Ca ++ rare
Most are isointense with cord on T1 – and T2WI
Moderate contrast enhancement
+/- dural "tail"

C. Other
Epidermoid cyst
Dermoid cyst
Tethered Cord
Low lying conus with or without a lipomas. Exiting nerve roots have a transverse or uphill course. Fibrous band can sometimes be seen in axial plane.

D. Malignant – Carcinomatous meningitis
Imaging findings
1. Nodular or plaquelike deposits intimately related to the conus and cauda equina
2. Focal, discrete lumbosacral mass lesions
3. Clumping and crowding of diffusely thickened lumbar nerve roots, causing a striated myelographic appearance
4. Root sleeve obliteration, sometimes with expansion of the axilla and ganglion caused by tumor implants

E. Diffusely thickened nerve roots
Common
Carcinomatous meningitis
Lymphoma
Leukemia
Uncommon
Toxic neuropathy
Neuritis
Multiple nerve root tumors (usually nodular)
Rare
Sarcoidosis
Histiocytosis

Intramedullary Tumors

A. Spinal ependymoma
    Histology and location
        Cellular ependymoma (anywhere, but usually cervical cord)
        Myxopapillary ependymoma (exclusively in conus medullaris and cauda equina)
    Most common spinal cork tumor overall; most common intramedullary tumor of adults
    Usually in middle-aged patients
    Conus ependymomas are slow-growing, may become extremely large and erode bone
    Imaging findings
        Vertebral body scalloping common with large conus lesions; may enlarge neural formina
        Hemorrhage common; cysts also frequent
        Usually isointense with cord on T1-, hyperintense on T2WI
        Enhances strongly, somewhat inhomogenously

B. Spinal cord astrocytoma
    Usually low-grade fibrillary astrocytoma; anaplastic astrocytoma, GBM rare
    Second most common spinal cord tumor overall; most common cord tumor in children
    Cause of low pain, pain, painful scoliosis in children
    Imaging findings
        Long, multisegment intramedullary mass typical, causes diffuse cord expansion
        Interpediculate distance widened, pedicles thinned
        Cysts common, often extensive
        Virtually 100 % enhance

C. Spinal cord hemangioblastoma

SUMMARY

INTRAMEDULLARY LESION

Tumors
- Ependymoma (most common, esp in adults)
- Astrocytoma (more common in children/Cx location)
- Medulloblastoma (CSF seeding)
- Lipoma/Dermoid/Epidermoid - especially in dysraphism
- Hemangioblastoma (Von Hippel-Lindau syndrome)
- Metastasis - breast/lung/melanoma
- Syringomyelia/Hydromyelia
- Hematoma Inflammation - myelitis
- AVM-Angioma

Cervical - usually glioma or syrinx
Thoracic - consider teratoma, dermoid, astrocytoma?

EXTRAMEDULLARY/INTRADURAL LESION

Meningioma (most thoracic)

Schwannoma (more common than neurofibroma)
Neurofibroma (erodes bone while extending through neural foramen, usually NF-1)
Drop metastasis - medulloblastoma/ependymoma/pineal dysgerminoma/glioma
Dermoid-Epidermoid (associated with dysraphism ?)
Lipoma - most common location is caudal (also "fatty filum")

COMMENT: Most tumors in this location are benign

EXTRADURAL LESION

Herniated disc (90% at L4-5 and L5-S1)
Osteophyte
Metastasis (Breast-Lung)
Lymphoma
Meningioma
Primary Bone tumor:
- Chordoma
- Osteosarcoma/blastoma
- Myeloma
- Aneurysmal bone cyst
- Giant cell tumor

Neurofibroma (often w/intradural component)
Dermoid-Epidermoid/Lipoma

SACRAL EXPANSILE LESION

Sacrococcygeal Teratoma (often presents in newborn)
Epidermoid cyst
Chordoma (bulky, lobulated mass with bone destruction)
Dural ectasia - meningocele
Dermoid
Lipoma
Giant cell tumor
Aneurysmal bone cyst

PEARLS IN THE DIAGNOSIS OF SPINAL ASTROCYTOMA

1. Thoracic location more common than cervical
   a. Astrocytoma is still the most common primary intramedullary malignant neoplasm of the cervical cord
   b. Ependymoma has a propensity for the lower thoracic and lumbar cord or conus
2. Poorly defined
3. Enhancement is variable but usually occurs less than six minutes after contrast administration
4. Hypointense T1 signal and hyperintense T2 signal
5. T2 signal hyperintensity is variable and mild to moderate
6. Lesion is cigar-shaped
7. On T1, patients who have myelitis may have a normal MR other than mild cord enlargement (and T2 is usually posterior lateral without mass effect in myelitis)
8. Patients with astrocytoma usually demonstrate discrete cord signal alteration

9. Myelitis tends to be less focal, more diffuse and more ill-defined than glioma (it may enhance, especially posterolaterally)
10. Gliomas may be extremely difficult to differentiate from glioma (usually there is a long-standing history of neurologic deficit)
11. Gliosis produces nominal to mild enhancement at best and usually associated with syrinx formation, scar formation or focal atrophy

PEARLS IN THE DIAGNOSIS OF SPINAL LYMPHOMA

- Bulky
- Relative bone sparing
- Insinuates itself in foramina and small spaces
- Enhancement is not as consistent as in the brain
- Propensity for posterior epidural spinal space
- Homogeneous
- May have adenopathy anteriorly

SPINE NEOPLASIA & SELECTED MASSES BY CONTRAST ENHANCEMENT

Intramedullary

- Ependymoma: Well-marginated, marked homogeneous enhancement
- Astrocytoma: Patchy, heterogeneous enhancement and more often eccentric compared to ependymoma
- Hemangioblastoma: Enhancement of a rounded nodule with nonenhancing surrounding cyst
- Cavernous hemangioma: No or nominal enhancement initially, delayed central enhancement
- Arteriovenous malformation: Heterogeneous enhancement admixed with flow void

Extramedullary Intradural

- Meningioma: Immediate, uniform, persistent enhancement
- Neurinoma: Homogeneous enhancement
- Drop metastases: Multifocal, rounded, nodular, enhancement

Extradural Lesions

- Metastases: Variable heterogeneous enhancement
- Arachnoiditis: Nominal to mild heterogeneous multifocal enhancement
- Disc extrusion: Minimal or moderate rimlike enhancement
- Meningocele: No enhancement
- Lymphoma: Homogeneous enhancement
- Abscess: Rim enhancement
- Synovial cyst: Rim enhancement
- Arthropathic pseudotumor: Mild diffuse enhancement

LEPTOMENINGEAL ENHANCEMENT & THICKENING

Focal

- Leptomeningeal carcinomatosis (e.g., breast, lung, melanoma): Lumpy
- Lymphoma: Lumpy or smooth
- Meningitis: Smooth
- Postoperative scarring: Smooth
- Subjacent acute infarction (pial collaterals): Smooth

Diffuse

- Leptomeningeal carcinomatosis (breast, lung, melanoma): Lumpy
- Meningitis (bacterial [common]; fungal and viral [rare]): Smooth
- Post radiation: Smooth
- Post shunt: Smooth
- Post subarachnoid hemorrhage: Smooth
- Post surgery: Smooth
- Post trauma: Smooth
- Sarcoidosis: Lumpy or smooth

Standard MRI Sequences for the Evaluation of Spinal Tumors [2]

T1-weighted image (T1WI) Spin echo	Excellent morphologic detail, especially cord size; dark CSF; important information about cysts, fat, blood
T2-weighted image (T2WI) Fast spin echo	FSE has mostly replaced spin echo T2; sensitive for identification of intramedullary tumor and edema; hyperintense CSF; susceptible to CSF motion artifacts, especially in axial plane in cervical spine
Gradient echo (GRE)	Sensitive to magnetic susceptibility artifact from hemorrhage; often used in axial plane in cervical spine instead of FSE T2 to reduce CSF pulsation artifact
T1-weighted + gadolinium	Useful for characterization and accurate assessment of borders of a lesion; distinguishes tumor from adjacent edema, and differentiates solid tumor from tumor cysts and syrinx; fat suppression improves contrast between enhancing lesion and background, distinguishes fat from hemorrhage, and is particularly important in extramedullary lesions

Special MRI Sequences in the Evaluation of Spinal Tumors [2]

FLAIR	CSF-suppressed T2-weighted sequence; intramedullary lesions may be less conspicuous on

	FLAIR than on FSE T2; CSF pulsation artifact accentuated
STIR	Fat-suppressed T2-weighted sequence; intramedullary lesions shown to be more conspicuous; particularly useful in assessment of trauma and infection; lower signal to noise than FSE T2; sensitive to motion
DWI	Currently limited in spine because of motion, spatial resolution, and susceptibility; in vivo application has been performed in spinal cord infarcts and MS
DTI	Application of DWI that measures diffusion anisotropy and may be used to trace white matter tracts; potential use in imaging spinal cord tumors, but not yet feasible in the clinical setting
MRS	Demonstrates spectrum of metabolites in region of interest; currently limited by spatial resolution and susceptibility artifacts and cannot yet be performed adequately in spine

Table 1. Summary of Spinal Tumors

Tumor	Location	Level	Frequency	Age (years)	Sex	Common Presentation	MRI Findings	Treatment
Ependymoma	Intramedullary	T, C	Most common intramedullary tumor	30–40	M=F	Local>radiating pain; 25% with bowel/bladder symptoms	Hypointense on T1, hyperintense on T2; homogeneous enhancement with cystic cap	Total excision ± radiation; recurrence common with subtotal excision
Astrocytoma	Intramedullary	T, C	2nd most common intramedullary	20–40	M=F	Local>radiating pain; often multiple vertebral levels; 30%–60% include cysts	Isointense on T1, hyperintense on T2; spinal cord enlargement, contrast enhancement	Excision ± radiation, chemotherapy
Cavernous malformation	Intramedullary	C, T	5% of intramedullary tumors (adults)	20–40	M=F	Motor deficit; acute progression (w/hemorrhage), chronic myelopathic progression	Mixed intensity on T1/T2; hypointense ring surrounding lesions	Excision
Hemangioblastoma	Intramedullary; rarely extramedullary or extradural	T, C	4% of spinal tumors; 25% patients have von Hippel-Lindau	20–30	M>F	Sensory/motor symptoms depending on location	Hypointense on T1, hyperintense on T2; appear as cysts with enhancing mural nodules; feeding vessels visible	Excision of symptomatic lesions
Ganglioglioma	Intramedullary	C, T	1% of spinal tumors	<15	M>F	Pain with radiculopathy, motor deficits	Isointense on T1, hyperintense on T2; heterogeneous enhancement	Excision, + radiation if subtotal resection
Lipoma	Extradural, extramedullary, or intramedullary	Varied	Rare	Before age 20	F>M	Sensory/motor symptoms with spinal dysraphism, cutaneous manifestations, tethered-cord syndrome	Hyperintense on T1 and T2	Excision if symptomatic; total excision preferred, not always feasible; treatment of neurologic deficits, foot deformities, etc. if syndromic
Subependymoma	Intramedullary	C>T	Rare	30–40	M>F	Often asymptomatic, discovered incidentally	Hypointense on T1, hyperintense on T2; heterogeneous enhancement	Excision, rarely chemotherapy or radiation
Oligodendroglioma	Intramedullary	T>L, C	Very rare	10–20	M=F	Sensory/motor symptoms depending on location	Isointense on T1, hyperintense on T2; appears as irregular mass with syrinx	Excision, if feasible ± radiation if advanced
Teratoma	Intramedullary	S, L, T, C	Rare	15–30	M=F	Pain, motor deficits, bladder dysfunction	Heterogeneous components with enhancement	Excision
Metastatic lesions	Extradural, rarely intramedullary	T>L>C	Most common source of extradural tumor	50–70	M=F	Local pain, symptoms from primary neoplasm	Often multiple foci	Radiation, chemotherapy, ± excision

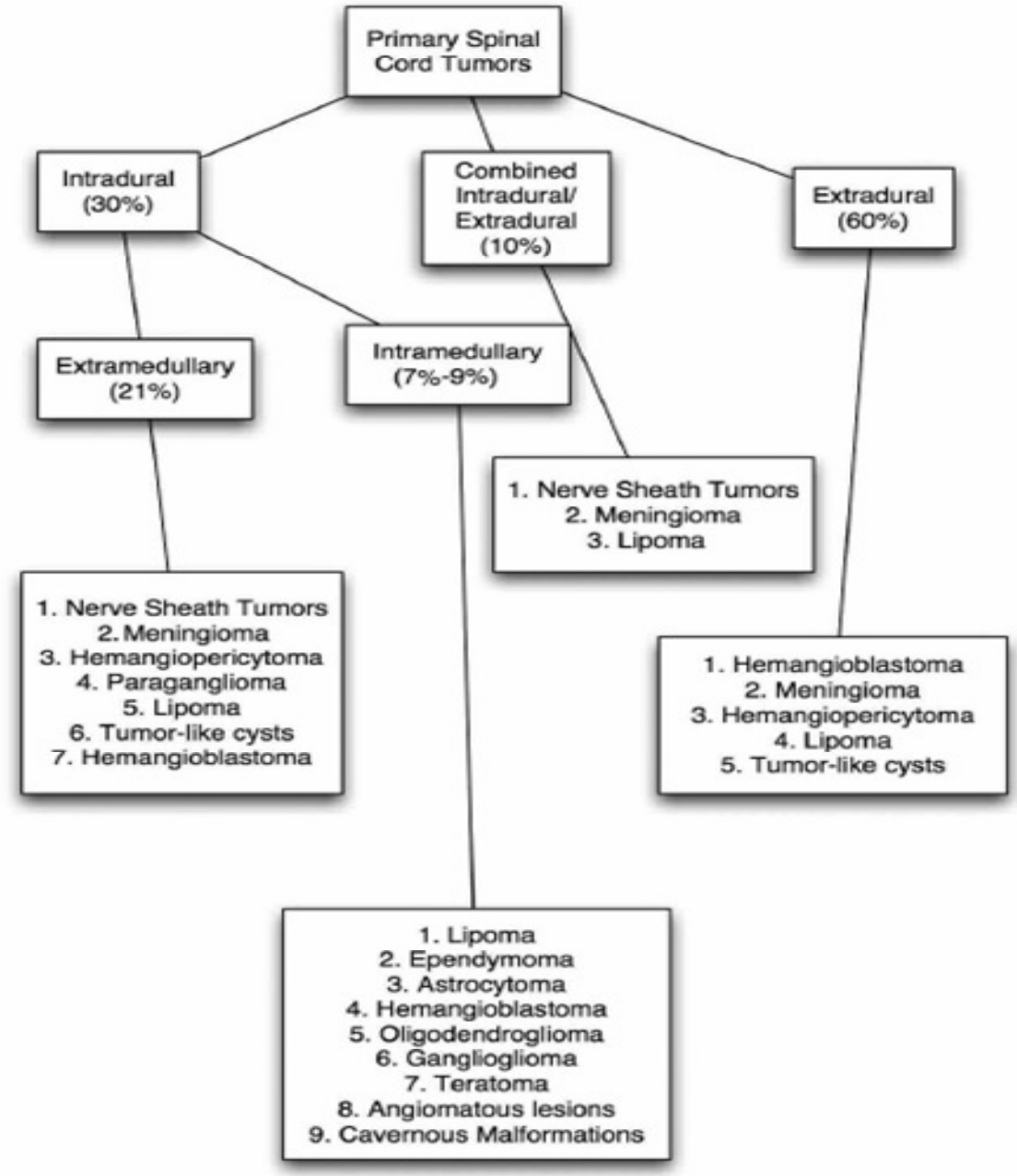

Flowchart of spinal tumors according to location.

REFERENCES

Bradley, WG, Daroff, RB, Fenichel, GM, and Marsden, CD. Neurology in Clinical Practice. Second Edition. Boston: 1996. vol. 2.

Kim, Daniel H, Chang, Ung-Kyu, Kim, Se-Hoon, and Bilsky, Mark H. Tumors of the Spine. First Edition. Philadelphia: Saunders-Elsevier; 2008. p. 185, 190.

Neurologic Clinics: Neuroimaging. Editor: Laszlo Mechtler, MD. Philadelphia: Saunders-Elsevier; Feb. 2009; 27(1).

Potts, EE and Capote, PM. *Neuroimaging of the Spine.* Continuum: Neuroimaging Aug. 2008; 14(4): 188-207.

Ross, Brant-Zawadzki, Moore, Crim, Chen, and Katzman. Diagnostic Imaging: Spine. First Edition. Salt Lake City: Arirsys; 2004.

Munns,J et al. Primary Spinal Cord Tumors. Contemporary Spine Surgery. Vol 10 2009